Histovariability and lifestyle in Proterochampsidae Romer, 1966 (Archosauriformes) from the Chañares Formation (Late Triassic), northwestern Argentina

Jordi Alexis GARCIA MARSÀ, Denis A. PONCE,
Federico Lisandro AGNOLÍN & Fernando E. NOVAS

Comptes Rendus Palevol est indexé dans / Comptes Rendus Palevol *is indexed by:*
– Cambridge Scientific Abstracts
– Current Contents® Physical
– Chemical, and Earth Sciences®
– ISI Alerting Services®
– Geoabstracts, Geobase, Georef, Inspec, Pascal
– Science Citation Index®, Science Citation Index Expanded®
– Scopus®.

Les articles ainsi que les nouveautés nomenclaturales publiés dans *Comptes Rendus Palevol* sont référencés par /
Articles and nomenclatural novelties published in Comptes Rendus Palevol *are registered on:*
– ZooBank® (http://zoobank.org)

Histovariability and lifestyle in Proterochampsidae Romer, 1966 (Archosauriformes) from the Chañares Formation (Late Triassic), northwestern Argentina

Jordi Alexis GARCIA MARSÀ
Laboratorio de Anatomía Comparada y Evolución de los Vertebrados,
Museo Argentino de Ciencias Naturales "Bernardino Rivadavia",
470 Ángel Gallardo, 1405DJR Buenos Aires (Argentina)
and CONICET, Avenida Ángel Gallardo 470, 1405DJR Buenos Aires (Argentina)
jagmdarwinista@gmail.com (corresponding author)

Denis A. PONCE
Instituto de Investigación en Paleobiología y Geología (IIPG), CONICET-Universidad Nacional
de Río Negro, Avenida J.A. Roca 1242, 8332 General Roca, Río Negro (Argentina)
and Museo 'Carlos Ameghino', Belgrano 1700, Paraje Pichi Ruca (predio Marabunta),
8300 Cipolletti, Río Negro (Argentina)
denispunrn@yahoo.com.ar

Federico Lisandro AGNOLÍN
Laboratorio de Anatomía Comparada y Evolución de los Vertebrados,
Museo Argentino de Ciencias Naturales "Bernardino Rivadavia",
470 Ángel Gallardo, 1405DJR, Buenos Aires (Argentina)
and CONICET, Avenida Ángel Gallardo, 470, 1405DJR, Buenos Aires (Argentina)
and Fundación de Historia Natural "Félix de azara",
Universidad Maimómides, 775 Hidalgo, Buenos Aires (Argentina)
fedeagnolin@yahoo.com.ar

Fernando E. NOVAS
Laboratorio de Anatomía Comparada y Evolución de los Vertebrados,
Museo Argentino de Ciencias Naturales "Bernardino Rivadavia",
470 Ángel Gallardo, 1405DJR Buenos Aires (Argentina)
and CONICET, Avenida Ángel Gallardo, 470, 1405DJR Buenos Aires (Argentina)
fernovas@yahoo.com.ar

ABSTRACT

This present work reports new data on the palaeohistology of Chañares Formation (early Carnian) proterochampsids based on appendicular bones, particularly *Chanaresuchus bonapartei* Romer, 1971 (i.e., PULR-V 116, femur, tibia and fibula) and *Tropidosuchus romeri* Arcucci, 1990 (i.e., PVL-4606, femur), and provides new insights into their paleobiology, histovariability, as well as lifestyle. *Chanaresuchus bonapartei* presents intraspecific and interelemental histovaribility with collagen fibers

organized from lamellar to woven fibered bone tissue, and degree of vascular density from sparse to dense. Both specimens appear to have attained sexual and skeletal maturity, but somatic maturity could not be inferred. *Tropidosuchus romeri* presents intraspecific histovariability with collagen fibers organized from parallel-fibered to woven fibered bone tissue, and dense vascularization. The lifestyle analysis for *T. romeri*, using a statistical model that employs anatomical and microanatomical data, suggests a terrestrial habit. The Proterochampsidae Romer, 1966 recovered from the Chañares Formation exhibits a large disparity in growth strategies among individuals of the same taxa, and with respect to other contemporaneous Archosauriformes.

RÉSUMÉ
Histovariabilité et mode de vie chez les Proterochampsidae Romer,1966 (Archosauriformes) de la formation Chañares (Trias supérieur), Nord-Ouest de l'Argentine.
L'objectif du présent travail est de présenter de nouvelles données sur la paléohistologie des protérochampsidés de la formation de Chañares (début du Carnien) en se basant sur les os appendiculaires, en particulier *Chanaresuchus bonapartei* Romer, 1971 (i.e., PULR-V 116, fémur, tibia et péroné) et *Tropidosuchus romeri* Arcucci, 1990 (i.e., PVL-4606, fémur), et de fournir de nouvelles informations sur leur paléobiologie, leur histovariabilité, ainsi que leur mode de vie. *Chanaresuchus bonapartei* présente une histovariabilité intraspécifique et interélémentaire avec des fibres de collagène organisées en tissu osseux lamellaire ou tissé, et un degré de densité vasculaire allant de clairsemé à dense. Les deux spécimens semblent avoir atteint la maturité sexuelle et squelettique, mais la maturité somatique n'a pu être déduite. *Tropidosuchus romeri* présente une histovariabilité intraspécifique avec des fibres de collagène organisées en fibres parallèles jusqu'au tissu osseux tissé, et une vascularisation dense. L'analyse du mode de vie, à l'aide d'un modèle statistique qui utilise des données anatomiques et microanatomiques, suggère un mode de vie terrestre pour *T. romeri*. Les Proterochampsidae Romer, 1966 retrouvés dans la formation de Chañares présentent une grande disparité dans les stratégies de croissance entre les individus d'un même taxon et par rapport à d'autres Archosauriformes contemporains.

INTRODUCTION

Proterochampsidae Romer, 1966 was an endemic group of non-archosaur Archosauriformes Gauthier, 1986 from South America, with taxa recovered exclusively from Argentina and Brazil (Trotteyn *et al.* 2013). Their phylogenetic affinities were uncertain for decades, and have been recently considered as a possible stem to the crown group Archosauria Cope, 1869 (e.g. Sereno & Arcucci 1990; Dilkes & Sues 2009; Ezcurra *et al.* 2010; Dilkes & Arcucci 2012; Nesbitt *et al.* 2013; Trotteyn *et al.* 2013; Ezcurra *et al.* 2019; Trotteyn & Ezcurra 2020; Wynd *et al.* 2020).

Proterochampsidae had a restricted temporal range (Arcucci *et al.* 2019). Their origin, diversification, and disappearance occurred in a short period of time, almost entirely in the Carnian (237-227 Ma).

Proterochampsidae were quadrupedal forms, with an elongated, triangular snout, a distinctly cranially ornamented dorsally flattened head, and dorsally positioned orbits and nostrils (e.g. Reig 1959; Sill 1967; Bonaparte 1971; Romer 1971). These morphological features are similar to those of present-day crocodilians, and led several authors to suggest a probable aquatic lifestyle for proterochampsids (Reig 1959; Sill 1967; Bonaparte 1971, 1997; Romer 1971; Barberena 1982; Kischlat 2000; Hsiou *et al.* 2002). However, new stud-

ies call into question such life habit inferences (e.g. Cerda *et al.* 2015; Ponce *et al.* 2017, 2021; Arcucci *et al.* 2019; Leuzinger 2020; Ezcurra *et al.* 2021). Regarding the growth pattern of proterochampsids, the abundance of fibrolamellar bone tissue and occasionally complex vascular patterns in long bones indicate high growth rates comparable to some pseudosuchians and the avemetatarsalian archosaurs (Ricqlès *et al.* 2008; Werning 2013; Arcucci *et al.* 2019; Marsà *et al.* 2020; Ponce *et al.* 2021).

In order to expand the paleohistological knowledge of Proterochampsidae, several transverse sections of different hindlimb bones were extracted from two specimens recovered from the Chañares Formation: *Tropidosuchus romeri* Arcucci, 1990 and *Chanaresuchus bonapartei* Romer, 1971. To expand on knowledge about the lifestyle of this taxa, compactness analyses were run on two other specimens of *T. romeri* and *C. bonapartei,* previously studied by Marsà *et al.* (2020). Romer (1971) described *Chanaresuschus bonapartei* on the basis of several partially articulated skeletons. Arcucci (1990) described *Tropidosuchus romeri* on the basis of several articulated and mostly complete individuals.

The present study focuses on the importance of histovariability when carrying out paleohistological analyses (e.g. Gallina 2012; Woodward *et al.* 2014, 2015; Botha & Botha-Brink 2019; Atterholt *et al.* 2021). Another goal is to

FIG. 1. — Bone tissue samples extracted from mid-shaft of long bones of Proterochampsidae Romer, 1966 from La Rioja province, NW Argentina, Chañares Formation, Carnian (Late Triassic): **A**, *Chanaresuchus bonapartei* Romer, 1971 (PULR-V 116) femur, tibia and fibula in posterolateral view; **B**, *Tropidosuchus romeri* Arcucci, 1990 (PVL- 4606), femur in posteromedial view. **Arrows** indicate place of the mid-shaft extraction. Scale bar: A, 5 cm; B, 1 cm.

increase paleobiological data emphasising the possibility of a terrestrial life habit for Proterochampsidae (e.g. Cerda *et al.* 2015; Ponce *et al.* 2017, 2021; Arcucci *et al.* 2019; Leuzinger 2020; Marsà *et al.* 2020; Ezcurra *et al.* 2021). Previous studies are compared to further explore this topic (Ricqlès *et al.* 2008; Dilkes & Sues 2009; Botha-Brink & Smith 2011; Cerda *et al.* 2015; Ponce *et al.* 2017, 2021; Arcucci *et al.* 2019; Marsà *et al.* 2020).

MATERIAL AND METHODS

Samples extracted for osteohistological analysis from bone tissue in the midshaft of the long bones belong to: *Chanaresuchus bonapartei* specimen PULR-V 116 (consisting of a femur, tibia and fibula); *Tropidosuchus romeri* specimen PVL-4606 (consisting of one femur) (Fig. 1; Table 1). Samples included in the compactness analysis belong to the femora

TABLE 1. — General histological features of the studied taxa. Abbreviations: **FLB**, fibrolamellar bone tissue; **LAG**, line of arrested growth; **LB**, lamellar bone tissue; **LC**, laminar canals; **LO**, longitudinals canals; **PFB**, parallel-fibered bone; **RC**, reticular canals; **TB**, trabecular bone.

Specimen	Matrix	Vascularization	Growth marks	Marrow cavity
Femur *Chanaresuchus bonapartei* Romer, 1971 PULR-V116	PFB	LO	1 LAG	TB
Tibia *Chanaresuchus bonapartei* PULR-V116	LB	LO	1 LAG	TB
Fibula *Chanaresuchus bonapartei* PULR-V116	FLB	LO>RC>LC	3 LAGs	TB
Femur *Tropidosuchus romeri* Arcucci, 1990 PVL-4606	PFB	LC>LO	0 LAGs	free

of: *Chanaresuchus bonapartei* specimen PULR-V 125; *Tropidosuchus romeri* specimen PVL-4604. Both were previously studied and described osteohistologically by Marsà *et al.* (2020). All specimens were recovered from the Late Triassic (Carnian) Chañares Formation, at Los Chañares locality, La Rioja province, Northwestern Argentina.

Different anatomical features of the almost complete specimen PULR-V 116 allow its assignation to *Chanaresuchus bonapartei* species (Romer 1971; Trotteyn *et al.* 2013; Trotteyn & Ezcurra 2020). PULR-V 116 has a reduced antorbital fenestra and slit-like external nares, placed close to the dorsal part and distant from the tip of the snout. The parietals swing sharply outward posteriorly, the suspensory is far from the posterior margin of the occiput, the lateral fenestra is elongated anteroposteriorly, and the coanas are markedly elongated. PULR-V 116 shows the presence of a well-defined anterior tympanic recess, a long, well-defined anterior tympanic recess, a long, narrow interpterygoid vacuity exposing a thin parasphenoid rostrum, and wedge-shaped osteoderms that narrow anteriorly and widen posteriorly.

Specimen PVL-4606 is a nearly complete specimen, originally described by Arcucci (1990) and referred to *Tropidosuchus romeri*. The specimen shares a unique combination of derived characteristics with *T. romeri*. These characteristics include a relatively large orbit, a distally curved premaxilla, a subversely oriented quadrangular axis, a skull roof with ornamentation formed by longitudinal ridges, and markedly elongated cervical vertebrae distinct from the dorsal elements that display a parallelogram morphology in lateral view (Trotteyn *et al.* 2013).

The histovariability analysis of the long bones of *Chanaresuchus* and *Tropidosuchus* takes into account previous studies analysing these taxons (Ricqlès *et al.* 2008; Werning 2013; Marsà *et al.* 2020; Ponce *et al.* 2021).

Thin sections of *Chanaresuchus bonapartei* PULR-V 116 and *Tropidosuchus romeri* PVL-4606 were prepared following the method outlined by Chinsamy & Raath (1992). The bones were embedded in a clear epoxy resin (Araldite© GY 279, catalyzed with Aradur® hY 951) and left for 24 hours to set. They were cut into smaller blocks perpendicular to the long axis of the bone using a cut-off diamond tipped saw within a Ken 9025 grinding machine. One surface of each resin block was then affixed to a frosted petrographic glass slide using the same resin that was used for embedding and left to set for a further 24 hours. The sections were wet-ground to approximately 60 µm thick and polished using a Prazis APL-S polishing machine with abrasive papers of increasing grit size (P80, P120, P320, P400, P600, P1200, P1500, P2000, P3000).

Samples were studied using a Zeiss Axio Scope.A1 petrographic polarizing microscope under normal and polarized light regimes.

Vascularization in the samples has not been quantified. Therefore, the relative densities of vascular canals are assessed visually and described qualitatively. The terminology of Warshaw (2008) is followed, with modifications. The following three terms are used: 1) sparse vascularization, vascular canals are irregularly distributed, with avascular stretches between them that generally exceed three times the diameter of the canals; 2) moderate vascularization, vascular canals are more regularly distributed, with the distance between canals frequently less than three times the diameter of the canals; and 3) dense vascularization, vascular canals are separated from each other by less than the diameter of two canals.

For the terminology of growth marks and bone matrix, the nomenclature proposed by Francillon-Vieillot *et al.* (1990) is followed.

To test the lifestyle of *Chanaresuchus* and *Tropidosuchus*, the ternary statistical model (TSM herein and elsewhere) was applied. This model is based on linear discriminant analyses, originally developed for lissamphibian femora (Laurin *et al.* 2004), and later expanded to amniote femora (Quémeneur *et al.* 2013). The results of the test predict three possible states of lifestyle, defined as: 0 = aquatic; 1 = amphibious; and 2 = terrestrial. Laurin *et al.* (2004) defines each state by the relative amount of time spent in water: >90% for aquatic taxon, between 20% and 90% for amphibious taxon, and <20% for terrestrial taxon. The TSM has an 88% accuracy predicting lifestyle for amniote femurs (Quémeneur *et al.* 2013).

The TSM uses several parameters provided by Bone Profiler (Gônet *et al.* 2022), an R script offering a series of analyses that evaluate compactness in a bone section. For the TSM, the most used parameter from Bone Profiler is the "observed compactness" (OC), which is the proportion of a cross-sectional area in an element that includes compact bone (represented by a value between 0-1). Another parameter of interest is the modelled (or predicted) compactness (MC). MC analyses can be run in bones that exhibit good preservation, even when slightly deformed. In this MC analysis, bone is represented by the colour black, while spaces, cavities, and canals are shown in white.

The "compactness profile" consists of a sigmoid curve, which represents the distribution of bone compactness from the medullary centre towards the outer limit of the cortex of the bone section. The results of the sigmoid curve include: the slope at the curve inflection (S); the location of the curve inflection point on the x-axis (P); the lowest (Min) and
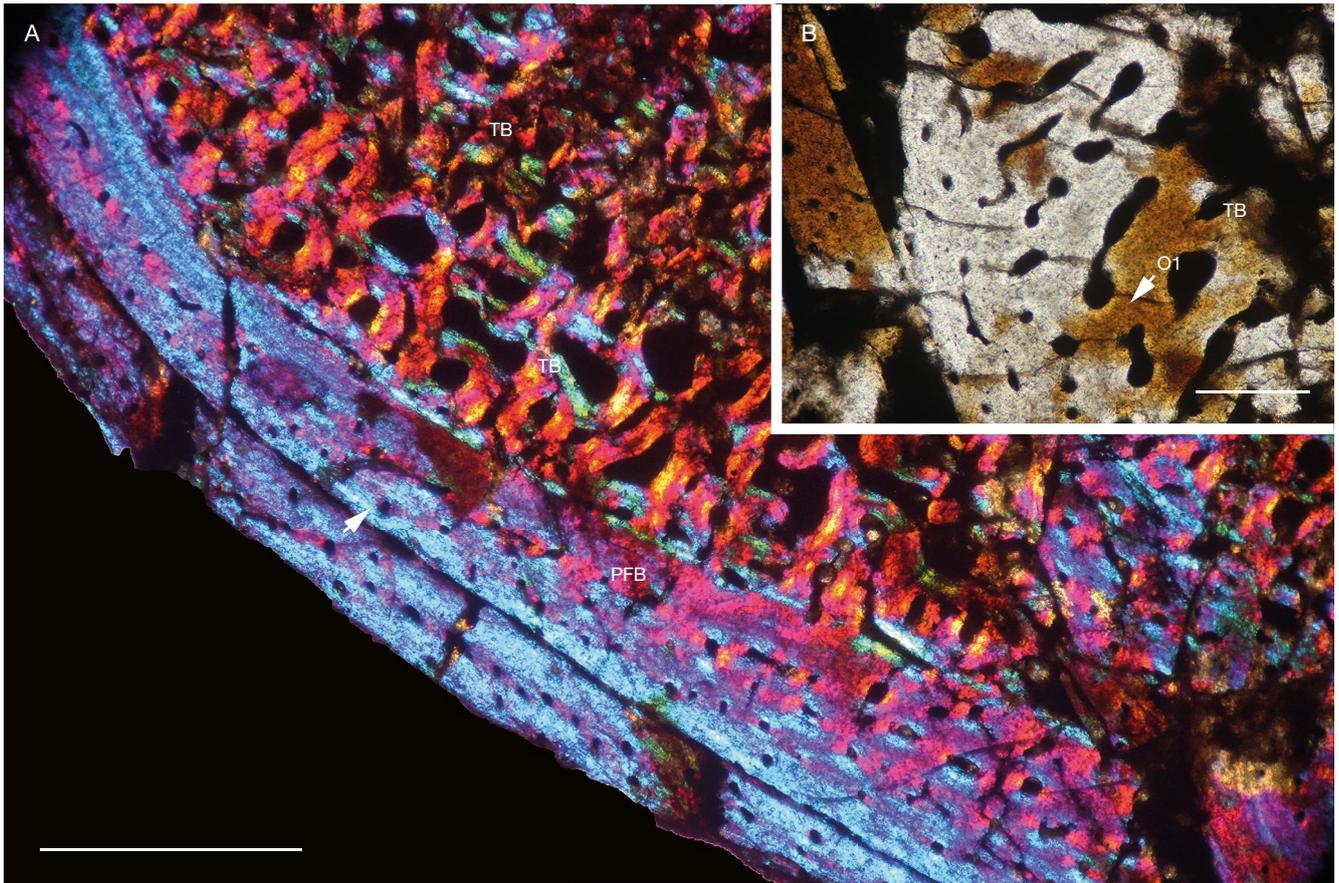
Fig. 2. — Femur of *Chanaresuchus bonapartei* Romer, 1971 (PULR-V 116): **A**, **B**, cross section in polarized light with lambda compensator showing the main features of the bone microstructure of the femur (**A**), where a LAG (**arrow**) is highlighted, and detail of the specimen (**B**) in normal light where the osteocyte lacunae can be distinguished as small subcircular punctations (**arrow**). Abbreviations: **O1**, primary osteons; **PFB**, parallel-fibered bone tissue; **TB**, trabecular bone. Scale bars: A, 1 mm; B, 250 µm.

highest (Max) value of compactness and its asymptote. Bone Profiler also provides angular analysis and its corresponding parameter values: radial slope (RS); radial inflection point (RP); radial minor (Rmin) and radial maximum (Rmax) value of compactness.

The TSM uses anatomical data from the "compactness profile" of Bone Profiler as well. Specifically the snout-vent length (SVL) (Quémeneur *et al.* 2013). For extinct taxa, the SVL is measured using the distance from the end of the snout to the posterior end of the sacrum.

To obtain a suitable "compactness profile" for the TSM, it is necessary that the section shows no (or very slight) deformation, and exhibits a good state of preservation. For this reason, the TSM was performed only in the femur of *Tropidosuchus romeri* PVL-4604, which meets these two criteria. For the SVL, it was only possible to measure *T. romeri* PVL-4604 from the original material. The low grade of deformation in the femur of *Chanaresuchus bonapartei* PULR-V 125 made it possible to obtain the compactness for this specimen, but not the "compactness profile". The femora of *C. bonapartei* PULR-V 116 and *T. romeri* PVL-4606 were not analyzed due to the high grade of deformation.

For more detailed explanation of the TSM model, and the global and angular parameters used, see Laurin *et al.* (2004)

and Quémeneur *et al.* (2013). Similar models have also been proposed to deduce lifestyle in extinct and extant tetrapods using other appendicular bones (Laurin *et al.* 2004; Germain & Laurin 2005; Kriloff *et al.* 2008; Canoville & Laurin 2009, 2010; Laurin & de Buffrénil 2016; Ponce *et al.* 2021).

ABBREVIATIONS

Institutional abbreviations

PULR-V   Colección Paleontología de Vertebrados, Universidad Nacional de La Rioja, La Rioja;
PVL   Colección Paleontología de Vertebrados Lillo, Universidad Nacional de Tucumán, San Miguel de Tucumán.

Other abbreviations

ATZ   avascular transition zone;
CCCB   compacted coarse cancellous bone;
EFS   external fundamental system;
FLB   fibro-lamellar bone tissue;
ICL   inner circumferential layer;
LAG   lines of arrested growth;
LB   lamellar bone tissue;
Max   highest value of compactness and its asymptote;
MC   modelled (or predicted) compactness;
Min   lowest value of compactness and its asymptote;
OC   observed compactness;
P   location of the curve inflection point on the x-axis;
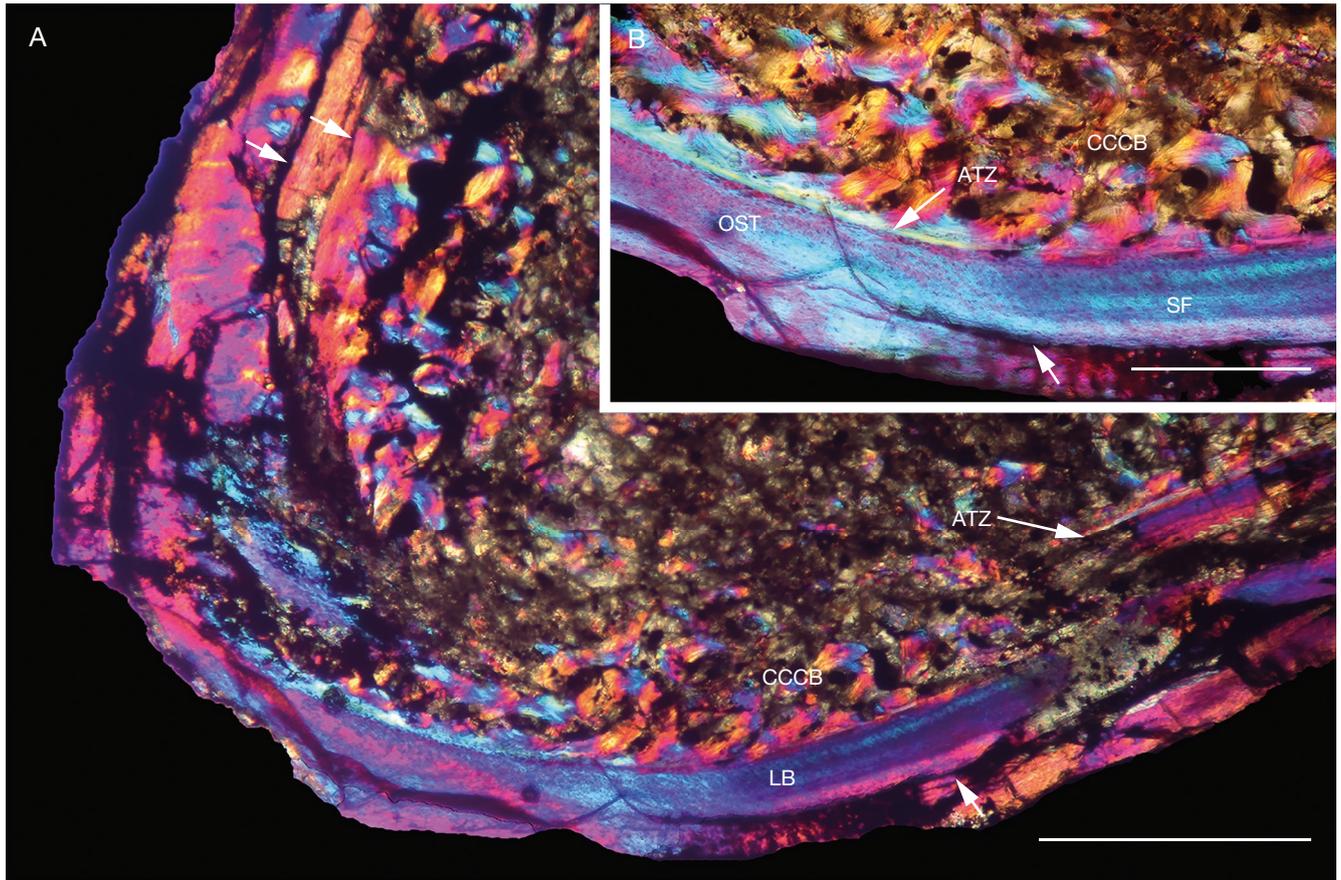
Fig. 3. — Tibia of *Chanaresuchus bonapartei* Romer, 1971 (PULR-V 116, polarized light with lambda compensator): **A**, **B**, cross section showing the main features of the bone microstructure of the tibia (**A**), highlighting the LAG (**arrows**), and detail of the specimen (**B**), where the osteocyte lacunae are visible as small subcircular punctae embedded in the avascular cortex. Abbreviations: **ATZ**, avascular transition zone; **CCCB**, compacted coarse cancellous bone; **LB**, lamellar bone tissue; **OST**, osteocyte lacunae; **SF**, Sharpey's fibers. Scale bars: A, 1 mm; B, 250 μm.

PFB   parallel-fibered bone tissue;
Rmax   radial maximum value of compactness;
Rmin   radial minor value of compactness;
RP   radial inflection point;
RS   radial slope;
S   slope at the curve inflection;
SVL   snout-vent length;
TSM   ternary statistical model.

RESULTS

Femur (PULR-V 116)

The cross section of the bone has been affected by diagenetic processes, with a collapse of the cortical surface that partially infilled into the medullary cavity. The diagenetic alterations do not affect the main features of bone microstructure.

The cortex is sparsely vascularized, in contrast to the femur of others specimens (Marsà *et al.* 2020; Ponce *et al.* 2021). The vascular canals are configured as longitudinally oriented primary osteons. The cortex is conformed by PFB and is interrupted by one LAG (Fig. 2A). Vascularization is very sparse, even null, in the subperiosteal area.

The medullary cavity is separated from the cortex by a resorption line, and it is infilled by a dense trabecular bone tissue, conformed by lamellar bone tissue.

The density of osteocyte lacunae across the cortex is low (Fig. 2B), contrasting with the high density of osteocyte lacunae present throughout the femoral cortex of other specimens (Marsà *et al.* 2020; Ponce *et al.* 2021). Their morphology ranges from circular to subcircular in both cortex and trabecular bone. The distribution between the osteocyte lacunae is equidistant.

Tibia (PULR-V 116)

The cross section of the bone has been affected by diagenetic processes, being fractured in several areas and collapsing towards the medullary cavity. However, these diagenetic alterations do not affect the main features of bone microstructure.

The cortex is almost avascular, with a few longitudinal canals, few secondary osteons, and interrupted by three LAGs (Fig. 3A). The cortex is constituted of LB and shows cyclical growth, with the presence of three LAGs. Some areas of the cortex present Sharpey's fibers.

The medullary cavity is infilled by a dense network of trabecular cancellous bone, tissue that is separated from the compact cortex by an ATZ (Fig. 3A, B), and conformed by lamellar bone tissue. Trabeculae are thicker than those described in the femur PULR-V 116.

The density of osteocyte lacunae is high (Fig. 3B), contrasting with the low density of osteocyte lacunae present along
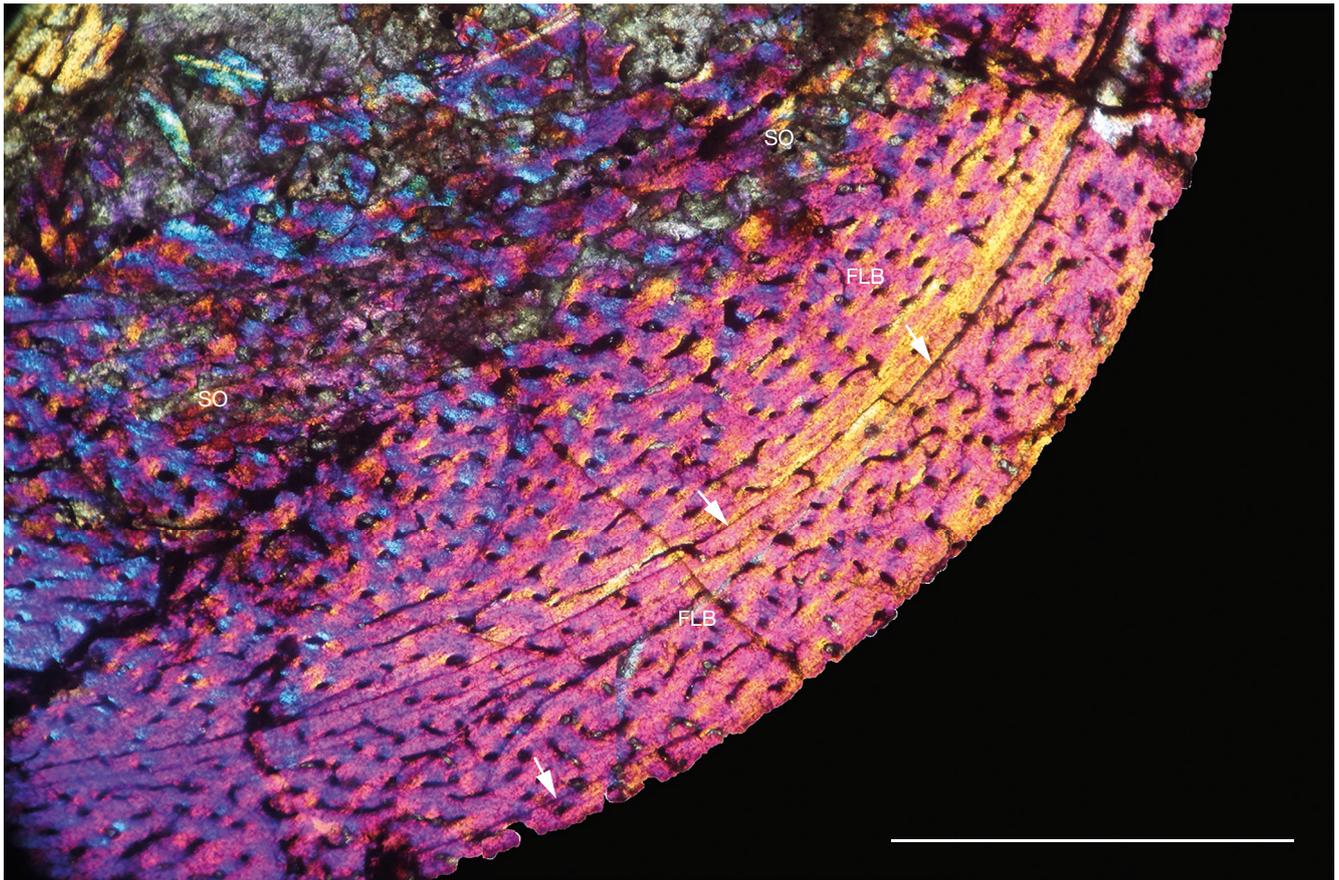
Fɪɢ. 4. — Fibula of *Chanaresuchus bonapartei* Romer, 1971 (PULR- V 116, in lambda light): cross section showing the main features of the bone microstructure of the fibula, highlighting the 3 LAGs (**arrows**). Abbreviations: **FLB**, fibrolamellar bone tissue; **SO**, secondary osteons. Scale bar: 2 mm.

the cortex of the femur PULR-V 116. These osteocyte lacunae are mostly circular in morphology, and orderly distributed. The osteocyte lacunae of the innermost cortex, adjacent to the CCCB, have a more elongated morphology.

Fɪʙᴜʟᴀ (PULR-V 116)

The cross section of the fibula has been affected by diagenesis, with the medullary cavity partially infilled by fragments of the cortex. But these diagenetic alterations do not affect the main features of bone microstructure.

The cortex is highly vascularized, in contrast to the femur and tibia of the same specimen (Fig. 4), resembling the femur of specimen PULR-V 125 (Marsà *et al.* 2020). The vascular canals are formed of primary osteons mostly longitudinally oriented, but some osteons exhibit a reticular pattern. A laminar arrangement of the primary osteons is also visible, but to a much lesser extent. In the inner cortex there are numerous secondary osteons. The half of the outer cortex closest to the subperiosteum consists of FLB and shows cyclical growth, with the presence of three LAGs (Fig. 4). Regarding the LAGs and their location in the FLB cortex: the first is a double LAG located at the middle of the FLB, and the last is located close to the subperiosteum. A thin layer of PFB forms around the LAGs.

The medullary cavity is reduced in comparison to the thickness of the cortex and infilled by trabecular bone tissue (Fig. 4).

A high density of osteocyte lacunae with oval morphology and irregular distribution are present throughout the cortex.

Fᴇᴍᴜʀ (PVL-4606)

The transverse section of the bone is well preserved, although part of the cortex collapsed and infilled inside the medullary cavity.

The cortex formed by PFB is densely vascularized (Fig. 5), even more than in the femur cortex of specimen PVL-4604 (Marsà *et al.* 2020). The vascular canals are mainly longitudinally and circumferentially arranged, which give rise to a laminar vascular organization (Fig. 5). Similar to PVL-4604 (Marsà *et al.* 2020), there is a reduction in the density of primary osteons towards the subperiosteum. The cortex is not interrupted by growth marks.

The medullary cavity is surrounded by a layer of lamellar bone tissue deposited endosteally, forming the ICL, which is thicker than in PVL-4604 (Marsà *et al.* 2020).

In this specimen the osteocyte lacunae are difficult to distinguish, probably due to diagenesis, and are less abundant than in *Chanaresuchus bonapartei* PULR-V 116 or *Tropidosuchus romeri* PVL-4604 (Marsà *et al.* 2020). The osteocyte lacunae
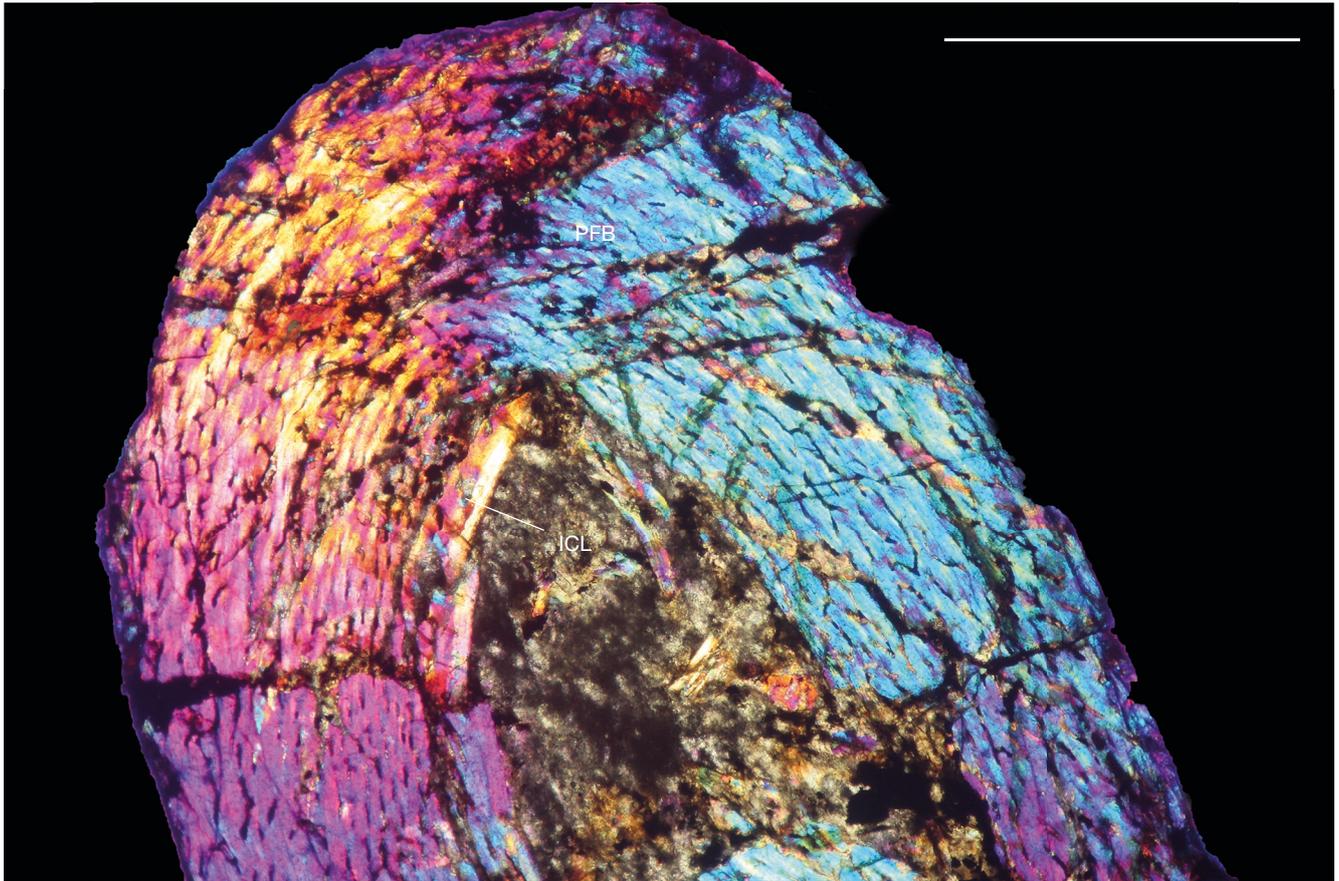
FIG. 5. — Femur of *Tropidosuchus romeri* Arcucci, 1990 (PVL-4606, in lambda light): cross section showing the main features of the bone microstructure of the femur. Abbreviations: **ICL**, inner circumferential layer; **PFB**, parallel-fibered bone tissue. Scale bar: 1 mm.
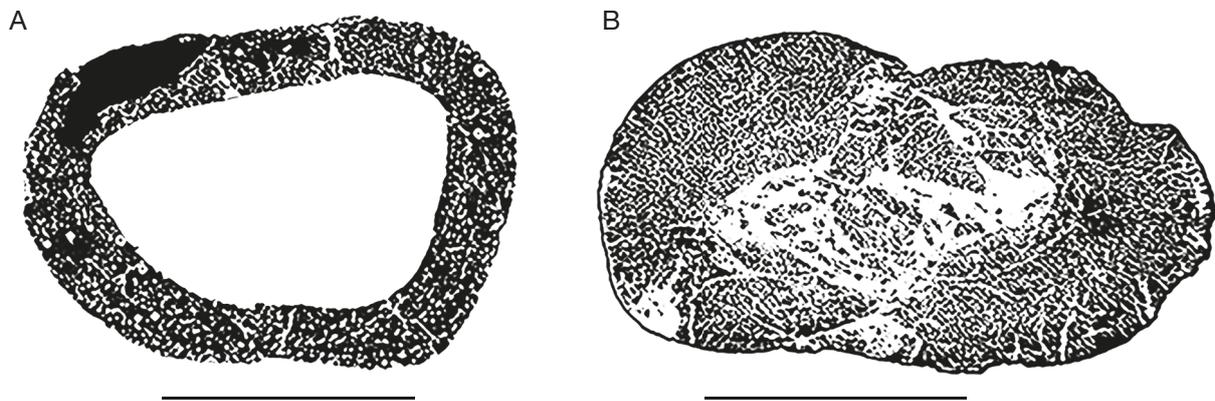
FIG. 6. — Observed compactness obtained from the proterochampsids sample. The analysis was done in sections which preserved a relatively complete portion of the whole bone element: **A**, femur of *Tropidosuchus romeri* Arcucci, 1990 PVL-4604, OC: 0.452; **B**, femur of *Chanaresuchus bonapartei* Romer, 1971 PULR-V 125; OC: 0.481. Scale bars: A, 500 μm; B, 1 mm.

are subcircular in outline and present throughout the cortex, as well as in the ICL, but in very low numbers in the latter.

COMPACTNESS ANALYSES

The OC was obtained for the femora of *Tropidosuchus romeri* (PVL-4604) and *Chanaresuchus bonapartei* (PULR-V 125) (Fig. 6). The rest of the samples are too cracked, fragmented or deformed to perform compactness analyses. The values of the observed compactness obtained for *T. romeri* (PVL-4604) and *C. bonapartei* (PULR-V 125) femora are 0.461 and 0.481 respectively.

The "compactness profile" and the TSM were obtained only in the femur of *T. romeri* (PVL-4604), because of its good state of preservation. The SVL results measure 24.4 cm.
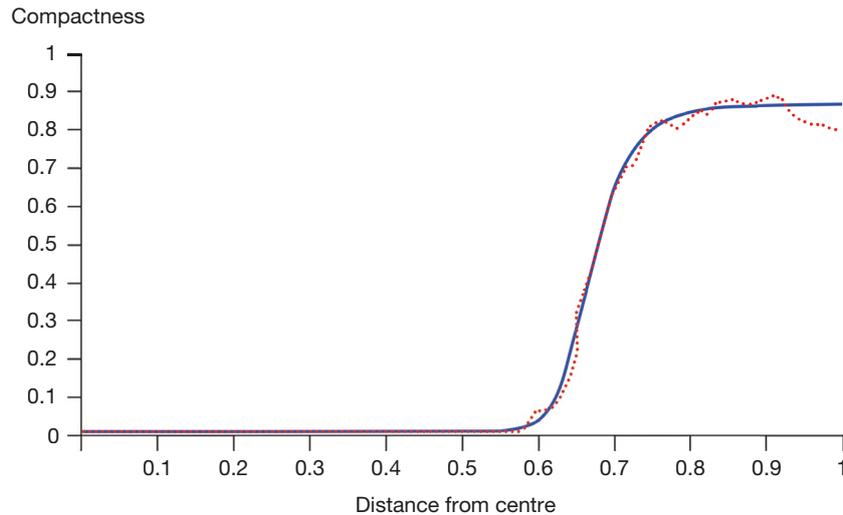
Fig. 7. — Compactness profile of *Tropidosuchus romeri* Arcucci, 1990 PVL-4604 femur of the transverse section performed with Bone Profiler. The P parameter at or near to 0.7 in "distance from the centre" indicates that the cortex occupies *c.* 0.3 (*c.* 30%) of the whole section. **Dotted curve** represents the trajectory of compactness through the section. The **solid curve** represents the results of the global values of the profile.

Table 2. — Compactness profile parameters of femur of *Tropidosuchus romeri* Arcucci, 1990 (PVL-4604), obtained by Bone Profiler (Gônet *et al.* 2022). Estimated snout-vent length: 244 mm. Abbreviations: **P**, location of the curve inflection point on the x-axis; **S**, slope at the curve inflection; **SD**, standard deviation.

Parameter	Mean global value	SD global value	Mean angular value	SD angular value
Min	0.000	0.000	0.000	0.000
Max	0.866	0.000	0.858	0.006
S: 1/slope	0.025	0.000	0.008	0.015
P: transition	0.670	0.000	0.665	0.061

The compactness profile is displayed in Figure 7, while the parameters from the compactness profile are summarized in Table 2. Using these data, the results of the TSM are state 2, a terrestrial lifestyle. Running of the TSM is available in the Appendix 1.

DISCUSSION

ONTOGENETIC STAGE
In bone tissues of tetrapods, a deceleration of the growth rate during the ontogeny of the individual is indicated by the following: reduced vascularization, predominance of longitudinal canals, lack of anastomoses, narrowing of zones deposited between successive lines of arrested growth, and formation of an external fundamental system at the bone perimeter (e.g. Horner *et al.* 1999; Horner *et al.* 2000; Padian & Horner 2004; Fostowicz-Frelik & Sulej 2010; Knoll *et al.* 2010; Marsà *et al.* 2017, 2020; Ponce *et al.* 2021). The *Tropidosuchus* and *Chanaresuchus* specimens studied here present several of these traits.

The femoral cortex of the specimen PULR-V 116 of *Chanaresuchus bonapartei* shows a very sparse vascularization subperiosteally (even absent in some areas) in comparison with the rest of the cortex, indicating a decrease in the growth rate.

The tibia of specimen PULR-V 116 shows a deceleration toward the subperiosteum similar to that recorded for the indeterminate long bone of *Chanaresuchus* sp. MCZ 4036 (Ricqlès *et al.* 2008), also indicating a decrease in the growth rate.

The fibular cortex of PULR-V 116 consists of fibrolamellar bone tissue than turns into parallel-fibered bone tissue subperiosteally, and registers a patent decrease in the number of vascular canals from the inner to the outer cortex, indicating an abrupt deceleration in the rate of bone deposition. The tibia and fibula are the elements with the highest number of growth marks, three LAGs each, which suggests a minimum age of three years for PULR-V 116, and are the most efficient for skeletochronology of the bone elements analyzed here. Nevertheless, when available, osteoderms give a better result for age determination because of the low degree of primary bone resorption evidenced in these elements (Ponce *et al.* 2021).

For the specimen PVL-4606 of *Tropidosuchus romeri*, the femoral cortex consists of parallel-fibered bone tissue. The decrease in the rate of bone deposition is indicated by the reduced vascularization recorded in the subperiosteum, in comparison to the rest of the cortex.

The different samples of proterochampsids studied here indicate that sexual maturity was reached before somatic and skeletal maturity. Sexual maturity (i.e., stage in which an individual is capable of breeding) is inferred by a decreasing rate in bone deposition and vascularization (Castanet & Baez

1991; Chinsamy-Turan 2005; Khonsue *et al.* 2010), which occurs in the specimens PULR-V 116 and PVL-4606. The absence of an external fundamental system in all the samples of *Chanaresuchus bonapartei* and *Tropidosuchus romeri* suggests that these elements have not attained somatic maturity (Woodward *et al.* 2011). However, we cannot rule out the postmortem destruction of the EFS.

Whereas sexual and somatic maturity can be determined by histological data (Erickson 2014), skeletal maturity is defined (and determined) using anatomical information (Brochu 1996). In the studied specimens, the neurocentral sutures are closed in the available cervical, dorsal, and caudal vertebrae. This indicates at least some degree of somatic and skeletal maturity, if this taxon follows the pseudosuchian fusion pattern, (which is caudal to cervical), as observed in modern crocodiles (Brochu 1996; Irmis 2007). However, the use of this proxy for extinct archosaurs not closely related to pseudosuchians might be debatable (Heinrich *et al.* 2021), due to the unknown ancestral status of Archosauria, and variations in timing and sequence orientation within the clade (Heinrich *et al.* 2021).

GROWTH PATTERNS

The evolution of bone growth rates and metabolic rates in Archosauromorpha von Huene, 1946 represent very active areas of research (e.g. Horner *et al.* 2000; Starck & Chinsamy 2002; Ricqlès *et al.* 2003; Padian *et al.* 2004; Erickson 2005; Ricqlès *et al.* 2008; Fostowicz-Frelik & Sulej 2010; Botha-Brink & Smith 2011; Griffin & Nesbitt 2016; Marsà *et al.* 2017, 2020; Ponce *et al.* 2017, 2021; Griffin *et al.* 2019; Veiga *et al.* 2019). Diverse works based on how the bone microstructure reflects growth rate, indicate that vascular density is closely linked to the rate of bone apposition (Amprino 1947; Padian & Horner 2004; Ricqlès *et al.* 2008).

The bone tissue of the proterochampsids *Tropidosuchus romeri* PVL-4606 and *Chanaresuchus bonapartei* PULR-V 116 seem to indicate a low growth rate. However, the formation of fibrolamellar bone tissue in the cortical matrix of Proterochampsidae is not unusual (Ricqlès *et al.* 2008; Arcucci *et al.* 2019; Marsà *et al.* 2020; Ponce *et al.* 2021), and in fact, suggests a rapid growth rate, significantly higher than in most non-archosaur Archosauriformes, and occasionally even archosaurs. The cortical matrix is typically associated with longitudinal vascular canals, although radial and laminar canals have also been recorded, especially in *C. bonapartei* (Marsà *et al.* 2020; Ponce *et al.* 2021). Cyclicity was not recorded on the cortical surface of *T. romeri*, but it was recorded in *C. bonapartei* (Ricqlès *et al.* 2008; Marsà *et al.* 2020; Ponce *et al.* 2021). This combination of features was also documented in other proterochampsids (Arcucci *et al.* 2019; Ponce *et al.* 2021) and some archosaurs such as *Terrestrisuchus gracilis* (Crush, 1984) and *Postosuchus kirkpatricki* (Chatterjee, 1985), as well as in Dinosauriformes Novas, 1992 (Ricqlès *et al.* 2003, 2008; Padian & Horner 2004). It should be noted that proterochampsid specimens normally show less vascularization in their cortex than dinosaurs (Horner *et al.* 2000; Starck & Chinsamy 2002; Ricqlès *et al.* 2003; Padian & Horner 2004), being closer to the basal

pterosauromorph *Lagerpeton chanarensis* Romer, 1971 and *Dromomeron romeri* Irmis, Nesbitt, Padian, Smith, Nathan, Turner, Woody & Downs, 2007 (Griffin *et al.* 2019; Marsà *et al.* 2020), as well as to non-dinosaur Dinosauriformes (Fostowicz-Frelik & Sulej 2010; Griffin & Nesbitt 2016; Marsà *et al.* 2017; Ezcurra *et al.* 2019; Veiga *et al.* 2019).

The fibula of *Chanaresuchus bonapartei* PULR-V 116 shows similarities with the indeterminate proterochampsid femora CRILAR-PV 603 and PULR-V 118 analyzed by Arcucci *et al.* (2019), with the femur of *C. bonapartei* PULR-V 125 (Marsà *et al.* 2020), and with the femur PVL 4575 and humerus CRILAR-Pv 81 of *C. bonapartei* analyzed by Ponce *et al.* (2021). These similarities are found in the vascularization patterns, growth marks and fibrillar organization.

The microstructural features of the shaft of the femur and tibia of *Chanaresuchus bonapartei* PULR-V 116 resemble samples studied by Arcucci *et al.* (2019). However, the Arcucci *et al.* (2019) samples were taken from the metaphyses and epiphyses, which usually correspond to areas strongly modified by bone remodeling processes. Finally, the *C. bonapartei* PULR-V 116 tibia and fibula exhibit lower growth rates than those found in specimens of *Tropidosuchus romeri*.

Tropidosuchus romeri shows significant intraspecific variation in the femoral microstructure. The femur of specimen PVL-4606 differs from PVL-4604 by having more complex vascularization in a large portion of its cortex, with laminar vascular canals, which would indicate a higher rate of bone deposition than the dominant longitudinal canals in PVL-4604 (Marsà *et al.* 2020). It is notable that the cortical matrix in PVL-4606 consists of parallel-fibered bone tissue, while in PVL-4604 it consists of fibrolamellar bone tissue which turns into parallel-fibered tissue subperiosteally (Marsà *et al.* 2020).

The presence of fibrolamellar bone tissue is shared by some samples of *Chanaresuchus bonapartei* (including PVL 4575), *Tropidosuchus romeri*, the indeterminate proterochampsids analyzed by Arcucci *et al.* (2019), and the unnamed Rhadinosuchinae Hofstetter, 1955 studied by Ponce *et al.* (2021). The diversity of vascularization patterns and bone tissues suggest a significant variation in growth patterns in the Proterochampsidae, an important part of these variable features are justifiable by different ontogenetic stages, as well as by developmental plasticity and/or sexual dimorphism. This clade of Archosauriformes records a great deal of interelemental and intraspecific histovariability, at least for *C. bonapartei* and *T.romeri*.

The growth patterns described for Proterochampsidae from the Chañares Formation show differences and similarities with those reported for other Archosauromorpha, such as those from the Triassic faunas of the Karoo Supergroup in South Africa (Botha-Brink & Smith 2011). For instance, the growth pattern of the prolacertiform archosaurmorph *Prolacerta brommi* Parrington, 1935 from the Lower Triassic, which exhibits a vascular pattern with longitudinally oriented primary osteons, anastomoses in some vascular canals, and the prevalence of a mixture of parallel-fibered bone tissue with scarcer fibrolamellar tissue (Botha-Brink & Smith 2011). Taking into account proterochampsid histovariability (Marsà *et al.* 2020; Ponce

et al. 2021), there are several histological features of *P. brommi* that resemble specimens of *Chanaresuchus* and *Tropidosuchus*.

The medium-sized proterosuchid *Proterosuchus fergusi* Broom, 1903, also recovered from the Karoo Supergroup, has radial vascular canals that are distributed in a cortical matrix of fibrolamellar bone tissue during early ontogeny, and a dramatic decrease in growth during late ontogeny, denoted by the presence of poorly vascularized lamellar bone tissue (Botha-Brink & Smith 2011). This contrasts with the proterochampsids from the Chañares Formation that generally show more active growth (although the poor vascularization associated with marked cyclicity and slow-depositional tissues recorded for the femur and tibia of *Chanaresuchus bonapartei* PULR-V 116 must be taken into account).

The erythrosuchid *Erythrosuchus africanus* Broom, 1905 of the Middle Triassic was described ostehistologically by several authors (Gross 1934; Ricqlès 1976; Ricqlès *et al.* 2008; Botha-Brink & Smith 2011). *Erythrosuchus africanus* exhibits uninterrupted growth of fibrolamellar bone tissue and a high variety of vascular patterns, including laminar, reticular, and radial canals, indicating accelerated growth rates similar to those found in fast-growing dinosaurs. *Garjainia madiba* Gower, Hancox, Botha-Brink, Sennikov & Butler, 2014, another erythrosuchid, from the Lower Triassic of the Karoo supergroup, exhibits growth patterns very similar to *E. africanus*, but its cortical surface is interrupted by annuli (Gower *et al.* 2014). Growth rates of *Tropidosuchus romeri* are lower than those of erythrosuchids. In some specimens of *Chanaresuchus bonapartei*, rapid growth is comparable to erythrosuchids, with a complex pattern of vascular canals and with cyclic growth similar to that of *Garjainia madiba*.

The euparkeriid archosauromorph *Euparkeria capensis* Broom, 1923, a contemporary of *Erythrosuchus africanus*, shows abundant vascular canals, quantitatively ranging from sparse to moderate, and a cortex constituted by parallel-fibered bone tissue (Botha-Brink & Smith 2011). *Euparkeria capensis* shows relatively low growth rates compared to some specimens of Proterochampsidae, nevertheless it is similar to the collagen fiber organization of *Tropidosuchus romeri* PVL 4606 and the less vascularized samples of *Chanaresuchus bonapartei* PULR-V 116.

Proterochampsidae of the Chañares Formation show marked differences in growth patterns in respect to *Vancleavea campi* Long & Murry, 1995, a Late Triassic proterochampsian (Ezcurra *et al.* 2010; Desojo *et al.* 2011; Ezcurra 2016; Trotteyn & Ezcurra 2020; Wynd *et al.* 2020). *Vancleavea campi* has a cortical surface of sparsely vascularized lamellar bone tissue (Nesbitt *et al.* 2009), only comparable to the microstructural features of the tibia of specimen PULR-V 116 of *Chanaresuchus bonapartei*.

Chanaresuchus bonapartei, *Tropidosuchus romeri*, the indeterminate proterochampsids studied by Arcucci *et al.* (2019), as well as the indeterminate Rhadinosuchinae, and *C. bonapartei* analyzed by Ponce *et al.* (2021) contrast microstructurally with the pseudosuchid *Gracilisuchus stipanicicorum* Romer, 1972, also recovered from Chañares Formation (Lecuona *et al.* 2020). Femoral analysis carried out by Lecuona *et al.*

(2020) revealed that the specimen died before reaching somatic maturity and that growth was relatively slow compared to other pseudosuchians. The predominance of poorly vascularized parallel-fibered bone tissue in the femur and osteoderms suggests a low growth rate, at least for this specimen. Bone matrix organization of *G. stipanicicorum* increases centrifugally with a simultaneous decrease in vascularization density, indicating a slowing of growth rate through ontogeny, despite no external fundamental system being recorded. In contrast to *G. stipanicicorum*, proterochampsids analyzed here show denser vascularizations and bone matrices usually associated with higher depositional rates. Taking into account proterochampsid histovariability (Marsà *et al.* 2020; Ponce *et al.* 2021), it cannot be ruled out that the growth pattern of *Gracilisuchus stipanicicorum* could be different in other specimens studied in the future.

The growth patterns of proterochampsids of the Chañares Formation exhibit the capacity to generate bone tissues of accelerated deposition and dense vascularization. Both these features are more accentuated than in some more derived taxa, such as pseudosuchians, at least during an important part of their ontogeny. These growth patterns would be plesiomorphic for Archosauriformes (Ricqlès *et al.* 2003, 2008; Fostowicz-Frelik & Sulej 2010; Marsà *et al.* 2017, 2020; Arcucci *et al.* 2019; Lecuona *et al.* 2020).

INTRA AND INTERELEMENTAL HISTOVARIABILITY

Intraelemental histovariability (within a particular bone of an individual) and interelemental histovariability (between different bone elements of the same individual) have been reported osteohistologically within the context of more general histological analyses (Chinsamy 1993; Curry 1999; Horner *et al.* 1999; Horner *et al.* 2000; Starck & Chinsamy 2002; Margerie *et al.* 2002, 2005; Ray & Chinsamy 2004; Botha-Brink & Chinsamy 2005; Ray *et al.* 2004, 2005; Gallina 2012; Woodward *et al.* 2014, 2015; Botha & Botha-Brink 2019; Atterholt *et al.* 2021). These analyses provide a useful background to better understand the underlying causes of intraelemental and interelemental histovariabilities.

Based on previous studies, interelemental histovariability can be attributed to asymmetric growth (e.g. Ray & Chinsamy 2004; Ray *et al.* 2004, 2005; Atterholt *et al.* 2021) or can be due to differences in the mode of ossification of the elements involved (periostial versus metaplastic ossification) (Gallina 2012).

Intraelemental variations are a product of the bone modelling, and in some cases, due to the fact that there are certain areas of the same element highly influenced by a superlative musculature, linked to trochanters, ridges, or bony scars generating histovariability (e.g. Botha-Brink & Chinsamy 2005; Gallina 2012).

It should be taken into account that general bone histology, and hence intra and interelemental histovariability, is affected by various factors, including phylogenetic, ontogenetic, functional, and biomechanical constraints (Ricqlès *et al.* 1991; Reid 1996; Curry 1999; Starck & Chinsamy 2002). Therefore, variation within the same skeleton should be expected.

In the femur of *Tropidosuchus romeri* PVL-4606 intraelemental histovariability is evident. The major axis of the bone on its anterior side has some longitudinal canals, which in the lateral and medial view turn into laminar canals. The areas with more complex vascularization correspond to accelerated growth, likely due to biomechanical limitations and bone modeling.

The intraelemental histovariability in *Chanareushcus bonapartei* PULR-V 116 is barely evident, but the interelemental histovariability between the elements of the hindlimb is remarkable. The femur and the tibia, with one and three LAGs respectively, show an arrangement of collagen fibers that form a parallel-fibered and lamellar bone matrix, respectively, with sparse vascularization in the femur and even more sparse in the tibia. Therefore, the femur has a higher growth rate compared to the tibia for the same time period. The most notable difference between all the elements is in the fibula, with fibrolamellar bone tissue and dense vascularization. Besides being interrupted cortically by three LAGs, the fibula has a greater cortical thickness in relation to the medullary cavity than the femur and tibia. This may be related with more juvenile stages (i.e., fast growing) in the fibula. The reduced medullary cavity of the fibula, in comparison to the other bones, is due to the tissues deposited early during the ontogeny, which are destroyed in the other bones during the expansion of the medullary cavity.

The most curious aspect of this histovariability, is that the element with the highest deposition rate, the fibula, also has one of the best records of cyclicity. The fibula is therefore, along with the tibia, the most efficient bone elements for skeletochronology, despite the fact that elements with less bone apposition typically give the best skeletochronological record.

Ponce *et al.* (2021) previously described interelemental histovariability between the femur and osteoderms for one specimen of *Chanaresuchus bonapartei* (PVL 4575), indicating that the most noticeable difference between the femoral and the osteodermal histology is the different LAG counts. This difference is due to the different growth rate for these elements.

To summarize, the interelemental histovariability in *Chanaresuchus bonapartei* PULR-V 116 shows elements indicative of both accelerated growth and slow growth. This points to the conclusion that *C. bonapartei* had high asymmetric growth in its skeletal elements.

DEVELOPMENTAL PLASTICITY:
INTRASPECIFIC HISTOVARIABILITY
Developmental plasticity is the ability of an individual to change its developmental patterns depending on environmental conditions (West-Eberhard 2003). Intraspecific histovariability is usually regarded as the result of evolutionary plasticity, however, there are other reasons for such variability, which may be inherent to each individual genotype; in any case it is typical that both possibilities contribute to intraspecific histovariability, even when epigenetics intervenes (e.g. Hochberg 2011; Kuzawa & Bragg 2012). For example, humans may grow to different degrees due to greater or lesser food availability, but they also often grow to different heights due to

genetic differences, independent of environmental pressure (e.g. Hochberg 2011; Kuzawa & Bragg 2012). This same phenomenon appears to have occurred in the temnospondyl *Apateon pedestris* von Meyer, 1844 (Sánchez *et al.* 2010).

Usually, in extant amniotes, strong developmental plasticity has been correlated with a low metabolic rate (Reisz *et al.* 2005), resulting in very different growth rates and final sizes in individuals of the same species, for example in turtles (Legler 1960; Zug *et al.* 1986), lizards (Dunham 1978; Zug & Rand 1987) and crocodiles (Cott 1961; Hutton 1986). However, this correlation does not seem to be consistent with the fossil record (e.g. Starck & Chinsamy 2002; Ricqlès *et al.* 2003; Padian *et al.* 2004; Ray *et al.* 2004, 2009; Chinsamy & Hurum 2006) or with other extant taxa, such as certain mammals and birds (Starck & Chinsamy 2002).

Previous comparative studies carried out in different groups of Archosauriformes, based on the histology of long bones, indicate that strong developmental plasticity is plesiomorphic for this clade, and has been maintained to the present in the crocodilian lineage (Padian *et al.* 2001; Ricqlès *et al.* 2003, 2008; Padian *et al.* 2004). Smith-Gill (1983), as well as Starck & Chinsamy (2002), indicate that the existence of LAGs is characteristic of developmental plasticity and the ability to respond to environmental changes, a pattern observed in diverse basal Archosauriformes and pseudosuchians (Ricqlès *et al.* 2003, 2008).

In contrast, ornithodirans (pterosauromorphs and dinosauroforms) are usually considered to have lost or greatly diminished developmental plasticity, based on the predominance of fibrolamellar bone tissue (Ricqlès *et al.* 2000, 2003; Padian *et al.* 2001; Starck & Chinsamy 2002; Padian *et al.* 2004). However, in certain taxa such as the basal sauropodomorph *Plateosaurus engelhardti* von Meyer, 1837, a strong developmental plasticity was attributed to a reversal to an ancestral condition (Sander & Klein 2005; Klein & Sander 2008). In other basals sauropodomorhps, such as *Massospondylus carinatus* Owen, 1854 and *Mussaurus patagonicus* Bonaparte & Vince, 1979, there is growing evidence of developmental plasticity (Chapelle *et al.* 2021; Cerda *et al.* 2022). This is reflected in the size of the adult individuals, which demonstrate a poor correlation between the body size and the ontogenetic stage for these taxa. These discrepancies may be related to sexual dimorphism and/or developmental plasticity (Chapelle *et al.* 2021; Cerda *et al.* 2022). This contrasts with the low variation observed in other basal dinosaurs such as *Herrerasaurus ischigualastensis* Reig, 1963 (Starck & Chinsamy 2002; Padian *et al.* 2004).

In this study, intraspecific histovariability was tested in proterochampsids. Although no growth marks were detected in femora in the two analyzed specimens of *Tropidosuchus romeri*, there are significant differences regarding the bone cortical tissues, despite having similar snout-vent lengths (25.2 cm for PVL-4604, and 24.4 cm for PVL-4606, respectively). The bone matrix in PVL-4604 is fibrolamellar (Marsà *et al.* 2020), indicating a high rate of bone deposition, while in PVL-4606 it is parallel-fibered, denoting a greater arrangement of collagen fibers and, therefore, a lower rate of bone deposition

than in PVL-4604. The vascularization in PVL-4606 is greater than in PVL-4604, and in some parts of the inner cortex the vascular canals are laminar, while in PVL-4604 the vascular canals are always longitudinal. These differences between the growth patterns could be related to sexual dimorphism and/or developmental plasticity (e.g. Cerda *et al.* 2022).

Regarding the specimens of *Chanaresuchus bonapartei*, the intraspecific histovariability among the analyzed femora is very pronounced. The cortical surface of the femur of *C. bonapartei* PULR-V 116 is poorly vascularized, in contrast to the femur of specimen PULR-V 125 (Marsà *et al.* 2020). The vascular canals in PULR-V 116 are formed as longitudinal primary osteons, while in PULR-V 125 they are reticular. In PULR-V 116 the cortex is thin, most of the total bone area in the section is trabecular bone, and it is constituted by parallel-fibered bone tissue, showing a cyclical growth, and the presence of one LAG. In PULR-V 125 the cortex is very thick, there are no traces trabeculae, and the zone of the cortex varies in some areas from parallel-fibered to fibrolamellar bone tissue, the cyclicity is constituted by a LAG and an annulus (Marsà *et al.* 2020).

The femur of PULR-V 125 resembles the femur of *Chanaresuchus bonapartei* PVL 4575 (Ponce *et al.* 2021), which is cortically composed of parallel-fibered bone tissue and some isolated areas of woven-fibered bone tissue. The vascularization is also similar, being composed of reticular and plexiform canals, and is only interrupted by a single LAG (Ponce *et al.* 2021). Both femora, PULR-V 125 and PVL 4575, are highly different from the femur PULR-V 116. Werning (2013) describes the histological tissues and vascularization of a femur from a possible *C. bonapartei*, specimen MCZ 4038, which closely resembles femora PULR-V 125 and PVL 4575: dense vascularization with reticular, woven-fibered bone in the inner cortex, and parallel-fibered bone tissue in the outer cortex. However, MCZ 4038 does not show growth marks, indicating another important instance of intraespecific histovariability.

The bone lengths of the femora of PULR-V 116 and PULR-V 125 are very similar, 7.1 cm and 7.3 cm respectively. This further supports that the differences between the growth patterns could be related to developmental plasticity and/or sexual dimorphism (e.g. Cerda *et al.* 2022) more than to ontogenic stages. Moreover, the bone length of the femora of PVL 4575 is 11.2 cm (Ponce *et al.* 2021), but has less growth marks than PULR-V 125, which is shorter. This reflects a poor correlation between the body size and the ontogenetic stage for this taxon (Chapelle *et al.* 2021; Cerda *et al.* 2022).

The lamelar bone tissue cortex of the tibia PULR-V 116 of *Chanaresuchus bonapartei* is almost avascular and interrupted by three LAGs. This contrasts sharply with the tibia of MCZ 4036, which has parallel-fibered bone tissue in the inner cortex, dominated by a dense reticular vascularization and interrupted by four LAGs, turning into lamellar bone tissue in the outer cortex, and associated with a decrease in the vascularization (Ricqlès *et al.* 2008). The bone length of the tibia of PULR-V 116 and MCZ 4036 are 9.3 cm and 12.9 cm respectively (Riclqès *et al.* 2008; Ponce *et al.* 2021).

These variations in bone tissue and length show a poor correlation between the body size and the ontogenetic stage, indicating developmental plasticity and/or sexual dimorphism (e.g. Cerda *et al.* 2022).

The high histovariability recorded in *Chanaresuchus bonapartei* and *Tropidosuchus romeri* suggests that associating intraspecific histovariability with developmental plasticity and/or sexual dimorphism would be typical in Proterochampsidae. Although developmental plasticity is usually associated with ectotherm animals (Reisz *et al.* 2005) that typically present slow growth, the Proterochampsidae analyzed occasionally exhibit the ability to generate bone tissues of accelerated deposition and complex patterns of vascularization.

LIFESTYLE INFERENCES IN PROTEROCHAMPSIDS

Reig (1959) proposed semi-aquatic habits for the proterochampsid *Proterochampsa barrionuevoi* Reig, 1959 based on morphological features resembling current crocodilians, including: elongated and triangular snout, dorsoventrally flattened head, profuse dermal ornamentation of the skull, and dorsally oriented external orbits and nostrils. This hypothesis was accepted by later authors and extrapolated to other members of the clade (Sill 1967; Romer 1971; Bonaparte 1978). Cerda *et al.* (2015) and Ponce *et al.* (2017), who studied the histology of proterochampsid osteoderms, favoured an aquatic or semi-aquatic lifestyle.

Several studies have indicated that modifications in the bone microanatomy of tetrapods are correlated with lifestyle (Ricqlès & Buffrénil 2001; Houssaye 2009). Living and extinct vertebrates secondarily adapted to aquatic life show four main types of bone tissue: osteoporotic, pachyostotic, osteosclerotic and pachyosteosclerotic (Ricqlès & Buffrénil 2001; Houssaye 2009). And in this sense, adaptation to aquatic life could be inferred on the basis of bone microstructure (Houssaye 2009; Canoville & Laurin 2010).

Nevertheless, recent studies reveal a more complex network of features shared by terrestrial and aquatic forms, and their habitat preference (Houssaye *et al.* 2016; Klein *et al.* 2019). For instance, dense and massive bones (i.e., with a high degree of compactness) are not always correlated with aquatic or semiaquatic lifestyle (Nakajima *et al.* 2014; Ponce *et al.* 2021). In this regard, more reliable lifestyle inferences should take into consideration both histological and anatomical features (Ponce *et al.* 2021).

Arcucci (2011) noted that the proterochampsids *Chanaresuchus bonapartei*, *Gualosuchus reigi,* and *Tropidosuchus romeri* may have possessed more terrestrial living habits than *Proterochampsa barrionuevoi*. Arcucci's (2011) proposal is based on the fact that the proterochampsids of the Chañares Formation (i.e., *C. bonapartei, G. reigi,* and *T. romeri*) display features atypical of aquatic taxa, such as the absence of a secondary palate, laterally compressed teeth, long and slender limbs, the absence of signs of reduction or enlargement of distal elements, subvertically positioned limbs, and a transversely broad, but not dorsoventrally high tail. However, some semi-aquatic forms, such as phytosaurs, also dispaly features typical of terrestrial taxa (e.g. no secondary palate, teeth are laterally

compressed; Nesbitt 2011). Similarly, Ezcurra *et al.* (2021) indicated that the tail of *C. bonapartei* was not an effective propellant in an aquatic environment, and therefore, there is no clear evidence to support a locomotor style associated with a semi-aquatic behavior.

Arcucci *et al.* (2019) reinforced their previous hypotheses and suggested terrestrial/amphibious living habits, based on, among other features, bone compactness and the presence of a reduced medullary cavity. Biogeochemical analyses of δ13C isotopes in the teeth and bones of proterochampsids also suggest terrestrial living habits for the Proterochampsidae (Leuzinger 2020).

Ponce *et al.* (2021) determined a terrestrial lifestyle for proterochampsids based on quantitative analysis of the femur. Such inferences are reinforced by the compactness observed in the femora of the proterochampsids *C. bonapartei* PVL 4575 and Rhadinosuchiade indet. (Ponce *et al.* 2021). The unnamed Rhadinosuchiade (Ponce *et al.* 2021) has an OC value of less than 0.50, which is similar to that reported for several terrestrial squamates, such as *Coleonyx elegans* Gray, 1845, *Gallotia stehlini* Schenkel, 1901, *Varanus rudicolis* Gray, 1845 and *Ameiva ameiva* Linnaeus, 1758 (± 0.1 variation from OC value: 0.5) (Hugi & Sánchez-Villagra 2012; Quémeneur *et al.* 2013). According to the database of Hugi & Sánchez-Villagra (2012) and Quémeneur *et al.* (2013), the amphibious lizard *Dracaena guianensis* Daudin, 1802 is the only taxon with a similar OC, but different lifestyle.

Following the previous studies of Ponce *et al.* (2021), and applying the TSM proposed by Quémeneur *et al.* (2013), the femur of *Tropidosuchus romeri* PVL-4604 has an observed compactness of less than 0.50 which is congruent with a terrestrial lifestyle. The observed compactness for the femora of *Chanaresuchus bonapartei* PULR-V 125 (OC: 0.481; see also Ponce *et al.* 2021), suggest a similar lifestyle.

CONCLUSIONS

The intraspecific histovariability in proterochampsids is remarkable. It appears that the intraspecific histovariability associated with developmental plasticity would be common in Proterochampsidae, and as Ezcurra *et al.* (2019) suggested, based on morphological features. Although developmental plasticity is usually associated with ectotherm animals (Reisz *et al.* 2005) that typically present slow growth, the Proterochampsidae analyzed occasionally exhibit the ability to generate bone tissues of accelerated deposition and complex vascularization. This ability is coincident with the plesiomorphic features for Archosaurifirmes (e.g. Ricqlès *et al.* 2003, 2008; Marsà *et al.* 2017, 2020; Veiga *et al.* 2019). It cannot be ruled out that an important part of the intraspecific histovariability could be related to sexual dimorphism, too. The interelemental histovariability in *Chanaresuchus bonapartei* is noticeable, which implies a high degree of asymmetric growth.

The compactness profile indicates a terrestrial lifestyle for *Tropidosuchus romeri*, congruent with most other proterochampsids lifestyle (Ponce *et al.* 2021).

The great disparity in growth strategies developed among the different Archosauriformes recovered from the Chañares Formation (Ricqlès *et al.* 2008; Werning 2013; Marsà *et al.* 2017, 2020; Arcucci *et al.* 2019; Lecuona *et al.* 2020; Ponce *et al.* 2021) resembles the analysis previously conducted by Botha-Brink & Smith (2011) for Lower and Middle Triassic Archosauromorphs from the Karoo Basin. They show that great disparity existed in growth strategies among contemporaneous taxa. These results contrast strongly with the geologically younger Ischigualasto Formation (Carnian-Norian) which shows a strong decrease in the disparity of growth strategies (Curry Rogers *et al.* 2017).

REFERENCES

AMPRINO R. 1947. — La structure du tissu osseux envisagée comme l'expression de differences dans la vitesse de l'accroissement. *Archives de Biologie* 58: 315-330.

ARCUCCI A. 1990. — Un nuevo Proterochampsia (Reptilia-Archosauriformes) de la fauna local de Los Chañares (Triásico Medio), La Rioja, Argentina. *Ameghiniana* 27 (3-4): 365- 378.

ARCUCCI A. 2011. — *Sistemática y Filogenia de los Proterochampsidos (Amniota, Diápsida, Archosauriformes) del Triásico de América del Sur, y sus Implicancias en el Origen de Archosauria*. PhD thesis, Universidad Nacional de San Luis, 336 p.

ARCUCCI A., PREVITERA E. & MANCUSO A. C. 2019. — Ecomorphology and bone microstructure of Proterochampsia from the Chañares Formation. *Acta Palaeontologica Polonica* 64 (1): 157-170. https://doi.org/10.4202/app.00536.2018

ATTERHOLT J., POUST A. W., ERICKSON G. M. & O'CONNOR J. K. 2021. — Intraskeletal osteohistovariability reveals complex growth strategies in a late Cretaceous enantiornithine. *Frontiers in Earth Science* 9: 640220. https://doi.org/10.3389/feart.2021.640220

BARBERENA M. C. 1982. — Uma nova espécie de *Proterochampsa, P. nodosa* sp. nov. do Triássico do Brasil. *Anais da Academia Brasileira de Ciências* 54: 127-141.

BONAPARTE J. F. 1971. — *Cerritosaurus binsfeldi* Price, tipo de una nueva familia de tecodontes (Pseudosuchia-Proterochampsia). *Anais da Academia Brasileira de Ciencias* 43: 417-422.

BONAPARTE J. F. 1978. — El Mesozoico de América del Sur y sus Tetrápodos. *Opera Lilloana* 26: 1-596.

BONAPARTE J. F. 1997. — *El Triásico de San Juan-La Rioja, Argentina, y sus Dinosaurios*. Museo Argentino de Ciencias Naturales, Buenos Aires, 190 p.

BOTHA-BRINK J. & CHINSAMY A. 2005. — Growth patterns of *Thrinaxodon*, a nonmammalian cynodont from the Early Triassic of South Africa. *Palaeontology* 48 (2): 385-394. https://doi.org/10.1111/j.1475-4983.2005.00447.x

BOTHA-BRINK J. & SMITH M. H. 2011. — Osteohistology of the Triassic archosauromorphs *Prolacerta*, *Proterosuchus*, *Euparkeria*, and *Erythrosuchus* from the Karoo Basin of South Africa. *Journal of Vertebrate Paleontology* 31 (6): 1238-1254. https://doi.org/10.1080/02724634.2011.621797

BOTHA A. E. & BOTHA-BRINK J. 2019. — Ontogenetic and interelemental osteohistological variability in the leopard tortoise *Stigmochelys pardalis*. *PeerJ* 7: e8030. https://doi.org/10.7717/peerj.8030

BROCHU C. A. 1996. — Closure of neurocentral sutures during crocodilian ontogeny: implications for maturity assessment in fossil archosaurs. *Journal of Vertebrate Paleontology* 16 (1): 49-62. https://doi.org/10.1080/02724634.1996.10011283

CANOVILLE A. & LAURIN M. 2009. — Microanatomical diversity of the humerus and lifestyle in lissamphibians. *Acta Zoologica* 90 (2): 110-122. https://doi.org/10.1111/j.1463-6395.2008.00328.x

CANOVILLE A. & LAURIN M. 2010. — Evolution of humeral microanatomy and lifestyle in amniotes, and some comments on palaeobiological inferences. *Biological Journal of the Linnean Society* 100 (2): 384-406. https://doi.org/10.1111/j.1095-8312.2010.01431.x

CASTANET J. & BÁEZ M. 1991. — Adaptation and evolution in Gallotia lizards from the Canary Islands: age, growth, maturity and longevity. *Amphibia-Reptilia* 12 (1): 81-102. https://doi.org/10.1163/156853891X00356

CERDA I. A., DESOJO J. B., TROTTEYN M. J. & SCHEYER T. M. 2015. — Osteoderm histology of Proterochampsia and Doswelliidae (Reptilia: Archosauriformes) and their evolutionary and paleobiological implications. *Journal of Morphology* 276 (4): 385-402. https://doi.org/10.1002/jmor.20348

CERDA I. A., POL D., OTERO A. & CHINSAMY A. 2022. — Palaeobiology of the early sauropodomorph *Mussaurus patagonicus* inferred from its long bone histology. *Palaeontology* 65 (4): e12614. https://doi.org/10.1111/pala.12614

CHAPELLE K. E., BOTHA J. & CHOINIERE J. N. 2021. — Extreme growth plasticity in the early branching sauropodomorph *Massospondylus carinatus*. *Biology Letters* 17 (5): 20200843. https://doi.org/10.1098/rsbl.2020.0843

CHINSAMY A. 1993. — Bone histology and growth trajectory of the prosauropod dinosaur *Massospondylus carinatus* Owen 1854. *Modern Geology* 18: 319-329.

CHINSAMY A. & RAATH M. A. 1992. — Preparation of fossil bone for histological examination. *Palaeontologia Africana* 29: 39-44.

CHINSAMY A. & HURUM J. H. 2006. — Bone microstructure and growth patterns of early mammals. *Acta Palaeontologica Polonica* 51 (2): 325-338.

CHINSAMY-TURAN A. 2005. — *The Microstructure of Dinosaur Bone*. The Johns Hopkins University Press, Baltimore, 195 p.

COTT H. B. 1961. — Scientific results of an enquiry into the ecology and economic status of the Nile crocodile (*Crocodylus niloticus*) in Uganda and Northern Rhodesia. *Transactions of the Zoological Society of London* 29 (4): 211-356. https://doi.org/10.1111/j.1096-3642.1961.tb00220.x

CURRY K. A. 1999. — Ontogenetic histology of *Apatosaurus* (Dinosauria: Sauropoda) new insights on growth rates and longevity. *Journal of Vertebrate Paleontology* 19 (4): 654-665. https://doi.org/10.1080/02724634.1999.10011179

CURRY ROGERS K., MARTINEZ R., ALCOBER O. & COLOMBI C. 2017. — *Comparative Bone Histology in the Ischigualasto Formation (Upper Triassic): Shedding Light on Early Dinosaur Growth Patterns*. Society of Vertebrate Paleontology, 77th Annual Meeting, Calgary, 101 p.

DESOJO J. B., EZCURRA M. D. & SCHULTZ C. L. 2011. — An unusual new archosauriform from the Middle-Late Triassic of southern Brazil and the monophyly of Doswelliidae. *Zoological Journal of the Linnean Society* 161 (4): 839-871. https://doi.org/10.1111/j.1096-3642.2010.00655.x

DILKES D. & ARCUCCI A. B. 2012. — *Proterochampsa barrionuevoi* (Archosauriformes: Proterochampsia) from the Late Triassic (Carnian) of Argentina and a phylogenetic analysis of Proterochampsia. *Palaeontology* 55 (4): 835-885. https://doi.org/10.1111/j.1475-4983.2012.01170.x

DILKES D. & SUES H. 2009. — Redescription and phylogenetic relationships of *Doswellia kaltenbachi* (Diapsida: Archosauriformes) from the Upper Triassic of Virginia. *Journal of Vertebrate Paleontology* 29 (1): 58-7. https://doi.org/10.1080/02724634.2009.10010362

DUNHAM A. E. 1978. — Food availability as a proximate factor in influencing individual growth rates in the iguanid lizard *Sceloporus merriami*. *Ecology* 59 (4): 770-778. https://doi.org/10.2307/1938781

ERICKSON G. M. 2005. — Assessing dinosaur growth patterns: a microscopic revolution. *Trends in Ecology and Evolution* 20 (12): 677-684. https://doi.org/10.1016/j.tree.2005.08.012

ERICKSON G. M. 2014. — On dinosaur growth. *Annual Review of Earth and Planetary Sciences* 42: 675-697. https://doi.org/10.1146/annurev-earth-060313-054858

EZCURRA M. D. 2016. — The phylogenetic relationships of basal archosauromorphs, with an emphasis on the systematics of proterosuchian archosauriforms. *PeerJ* 4: e1778. https://doi.org/10.7717/peerj.1778

EZCURRA M. D., LECUONA A. & MARTINELLI A. 2010. — A new basal archosauriform diapsid from the Lower Triassic of Argentina. *Journal of Vertebrate Paleontology* 30 (5): 1433-1450. https://doi.org/10.1080/02724634.2010.501446

EZCURRA M. D., von BACZKO M. B., TROTTEYN M. J. & DESOJO J. B. 2019. — New proterochampsid specimens expand the morphological diversity of the rhadinosuchines of the Chañares Formation (lower Carnian, northwestern Argentina). *Ameghiniana* 56 (2): 79-115. https://doi.org/10.5710/AMGH.25.05.2019.3230

EZCURRA M. E., NESBITT S. J., FIORELLI L. E. & DESOJO J. B. 2020. — New specimen sheds light on the anatomy and taxonomy of the Early Late Triassic dinosauriforms from the Chañares Formation NW Argentina. *The Anatomical Record* 303 (5): 1393-1438. https://doi.org/10.1002/ar.24243

EZCURRA M. D., MONTEFELTRO F. C., PINHEIRO F. L., TROTTEYN M. J., GENTIL A. R., LEHMANN O. E. & PRADELLI L. A. 2021. — The stem-archosaur evolutionary radiation in South America. *Journal of South American Earth Sciences* 105: 102935. https://doi.org/10.1016/j.jsames.2020.102935

FOSTOWICZ-FRELIK L. & SULEJ T. 2010. — Bone histology of *Silesaurus opolensis* Dzik, 2003 from the Late Triassic of Poland. *Lethaia* 43 (2): 137-148. https://doi.org/10.1111/j.1502-3931.2009.00179.x

FRANCILLON-VIEILLOT H., BUFFRÉNIL V. de, CASTANET J., GÉRAUDIE J., MEUNIER F. J., SIRE J. Y., ZYLBERBERG L. & RICQLES A. de 1990. — Microstructures and mineralization of vertebrate skeletal tissues, *in* CARTER J. (ed.), *Skeletal Biomineralizations: Patterns, Processes and Evolutionary Trends*. Vol. 1. Van Nostrand Reinhold, New York: 471-530.

GALLINA P. A. 2012. — Histología ósea del titanosaurio *Bonitasaura salgadoi* (Dinosauria: Sauropoda) del Cretácico superior de Patagonia. *Ameghiniana* 49 (3): 289-302. https://doi.org/10.5710/AMGH.v49i3(519)

GERMAIN D. & LAURIN M. 2005. — Microanatomy of the radius and lifestyle in amniotes (Vertebrata, Tetrapoda). *Zoologica Scripta* 34 (4): 335-350. https://doi.org/10.1111/j.1463-6409.2005.00198.x

GÔNET J., LAURIN M. & GIRONDOT M. 2022. — BoneProfileR: The next step to quantify, model, and statistically compare bone section compactness profiles. *Palaeontologia Electronica* 25 (1): a12. https://doi.org/10.26879/1194

Gower D. J., Hancox P. J., Botha-Brink J., Sennikov A. G. & Butler R. J. 2014. — A new species of *Garjainia* Ochev, 1958 (Diapsida: Archosauriformes: Erythrosuchidae) from the Early triassic of South Africa. *PLoS ONE* 9 (11): e111154. https://doi.org/10.1371/journal.pone.0111154

Griffin C. T. & Nesbitt S. J. 2016. — The femoral ontogeny and long bone histology of the Middle Triassic (?late Anisian) dinosauriform *Asilisaurus kongwe* and implications for the growth of early dinosaurs. *Journal of Vertebrate Paleontology* 36 (3): e1111224 https://doi.org/10.1080/02724634.2016.1111224

Griffin C. T., Bano L. S., Turner A. H., Smith N. D., Irmis R. B. & Nesbitt S. J. 2019. — Integrating gross morphology and bone histology to assess skeletal maturity in early dinosauromorphs: new insights from *Dromomeron* (Archosauria: Dinosauromorpha). *PeerJ* 7: e6331. https://doi.org/10.7717/peerj.6331

Gross W. 1934. — Die Typen des mikroskopischen Knochenbaues bei fossilen Stegocephalen und Reptilien. *Zeitschrift der Anatomie und Entwicklungsgeschichte* 103: 731-764. https://doi.org/10.1007/BF02118752

Heinrich C., Paes Neto V. D., Lacerda M. B., Martinelli A. G., Fiedler M. S. & Schultz C. L. 2021. — The ontogenetic pattern of neurocentral suture closure in the axial skeleton of Hyperodapedontinae (Archosauromorpha, Rhynchosauria) and its evolutionary implications. *Palaeontology* 64 (3): 409-427. https://doi.org/10.1111/pala.12528

Hochberg Z. 2011. — Developmental plasticity in child growth and maturation. *Frontiers in Endocrinology* 2: 41. https://doi.org/10.3389/fendo.2011.00041

Horner J. R., de Ricqlès A. J. & Padian K. 1999. — Variation in skeletochronological indicators of the hadrosaurid dinosaur *Hypacrosaurus*: implications for age assessment of dinosaurs. *Palaeobiology* 25 (3): 295-304. https://doi.org/10.1017/S0094837300021308

Horner J. R., Ricqlès A. de & Padian K. 2000. — Long bone histology of the hadrosaurid dinosaur *Maiasaura peeblesorum*: growth dynamics and physiology based on an ontogenetic series of skeletal elements. *Journal of Vertebrate Paleontology* 20: 115-129. https://doi.org/c8th29

Houssaye A. 2009. — Pachyostosis in aquatic amniotes: a review. *Integrative Zoology* 4 (4): 325-340. https://doi.org/10.1111/j.1749-4877.2009.00146.x

Houssaye A. 2013. — Palaeoecological and morphofunctional interpretation of bone mass increase: an example in Late Cretaceous shallow marine squamates. *Biological reviews of the Cambridge Philosophical Society* 88 (1): 117-139. https://doi.org/10.1111/j.1469-185X.2012.00243.x

Houssaye A., Sander P. M. & Klein N. 2016. — Adaptive patterns in aquatic amniote bone microanatomy – more complex than previously thought. *Integrative & Comparative Biology* 56 (6): 1349-1369. https://doi.org/10.1093/icb/icw120

Hsiou A., Adbala F. & Arcucci A. B. 2002. — Novo registro de Proterocampsídeo (Reptilia, Archosauriformes) do Triássico Médio-Superior do Brasil. *Revista Brasileira de Palentologia* 3: 48-55.

Hugi J. & Sánchez-Villagra M. R. 2012. — Life history and skeletal adaptations in the Galapagos marine iguana (*Amblyrhynchus cristatus*) as reconstructed with bone histological data – a comparative study of iguanines. *Journal of Herpetology* 46 (3): 312- 324. https://doi.org/10.1670/11-071

Huttenlocker A. K. & Botha-Brink J. 2013. — Body size and growth patterns in the therocephalian *Moschorhinus kitchingi* (Therapsida: Eutheriodontia) before and after the end-Permian extinction in South Africa. *Paleobiology* 39: 253-277. https://doi.org/10.1666/12020

Hutton J. M. 1986. — Age determination of living Nile crocodiles from the cortical stratification of bone. *Copeia* 2: 332-341. https://doi.org/10.2307/1444994

Irmis R. B. 2007. — Axial skeleton ontogeny in the Parasuchia (Archosauria: Pseudosuchia) and its implications for ontogenetic determination in archosaurs. *Journal of Vertebrate Paleontology* 27 (2): 350-361. https://doi.org/css9hq

Khonsue W., Chaiananporn T. & Pomchote P. 2010. — Skeletochronological assessment of age in the Himalayan crocodile newt, *Tylototriton verrucosus* (Anderson, 1871) from Thailand. *Tropical Natural History* 10: 181–188.

Kischlat E. E. 2000. — Tecodôncios: a aurora dos arcossáurios no Triássico, *in* Holz M. & de Ross L. F. (eds), *Paleontologia do Rio Grande do Sul*. CIGO/UFRGS, Porto Alegre: 273-316.

Klein N. & Sander P. M. 2008. — Ontogenetic stages in the long bone histology of sauropod dinosaurs. *Paleobiology* 34: 247-263. https://doi.org/dhzsf3

Klein N., Canoville A. & Houssaye A. 2019. — Microstructure of vertebrae, ribs, and gastralia of Triassic sauropterygians – new insights into the microanatomical processes involved in aquatic adaptations of marine reptiles. *The Anatomical Record* 302 (10): 1770-1791. https://doi.org/10.1002/ar.24140

Knoll F., Padian K. & Riqclès de A. 2010. — Ontogenetic change and adult body size of the early ornithischian dinosaur *Lesothosaurus diagnosticus*: implications for basal ornithischian taxonomy. *Gondwana Research* 17 (1): 171-179. https://doi.org/10.1016/j.gr.2009.03.010

Kriloff A., Germain D., Canoville A., Vincent P., Sache M. & Laurin M. 2008. — Evolution of bone microanatomy of the tetrapod tibia and its use in palaeobiological inference. *Journal of Evolutionary Biology* 21 (3): 807-826. https://doi.org/10.1111/j.1420-9101.2008.01512.x

Kuzawa C. W. & Bragg J. M. 2012. — Plasticity in human life history strategy: implications for contemporary human variation and the evolution of genus *Homo*. *Current Anthropology* 53 (56): 369-382. https://doi.org/10.1086/667410

Laurin M. & Buffrénil V. de 2016. — Microstructural features of the femur in early ophiacodontids: a reappraisal of ancestral hábitat use and lifestyle of amniotes. *Comptes Rendus Palevol* 15 (1-2): 115-127. https://doi.org/10.1016/j.crpv.2015.01.001

Laurin M., Girondot M. & Loth M. M. 2004. — The evolution of long bone microanatomy and lifestyle in lissamphibians. *Paleobiology* 30 (4): 589-613. https://www.jstor.org/stable/4096912

Lecuona A., Desojo J. B. & Cerda I. A. 2020. — New information on the anatomy and histology of *Gracilisuchus stipanicicorum* (Archosauria: Pseudosuchia) from the Chañares Formation (early Carnian), Argentina. *Comptes Rendus Palevol* 19 (3): 40-62. https://doi.org/10.5852/cr-palevol2020v19a3

Legler W. K. 1960. — *Natural History of the Ornate Box Turtle, Terrapene Ornata Ornata Agassiz*. Vol. 11. University of Kansas publications, Museum of Natural History, Lawrence: 527-669.

Leuzinger L. 2020. — *Estudio biogeoquímico de Arcosauromorpha del Mesozoico de La Rioja (Noroeste de Argentina): estado de preservación, paleoambientes y paleoecología*. PhD thesis, Universidad Nacional de Córdoba, Córdoba, 253 p.

Margerie de, Cubo J. & Castanet J. 2002. — Bone typology and growth rate: testing and quantifying "Amprino's rule" in the mallard (*Anas platyrhynchos*). *Comptes Rendus Biologies* 325 (3): 221-230. https://doi.org/10.1016/S1631-0691(02)01429-4

Margerie E. de, Sanchez S., Cubo J. & Castanet J. 2005. — Torsional resistance as a principal component of the structural design of long bones: comparative multivariate evidence in birds. *Anatomical Record* 282A (1): 49-66. https://doi.org/10.1002/ar.a.20141

Marsà J. A. G., Agnolín F. L. & Novas F. E. 2017. — Bone microstructure of *Lewisuchus admixtus* Romer, 1972 (Archosauria, Dinosauriformes). *Historical Biology* 31 (2): 157-162. https://doi.org/10.1080/08912963.2017.1347646

Marsà J. A. G., Agnolín F. L. & Novas F. E. 2020. — Comparative bone microstructure of three archosauromorphs from the Carnian, Late Triassic Chañares Formation of Argentina. *Acta Palaeontologica Polonica* 65: 387-398.

MARSICANO C. A., IRMIS R. B., MANCUSO A. C., MUNDIL R. & CHEMALE F. 2016. — The precise temporal calibration of dinosaur origins. *Proceedings of the National Academy of Sciences of the United States of America* 113 (3): 509-513. https://doi.org/10.1073/pnas.1512541112

NAKAJIMA Y., HIRAYAMA R. & ENDO H. 2014. — Turtle humeral microanatomy and its relationship to lifestyle. *Biological Journal of the Linnean Society* 112 (4): 719-734. https://doi.org/10.1111/bij.12336

NESBITT S. J. 2011. — The early evolution of archosaurs: relationships and the origin of major clades. *Bulletin of the American Museum of Natural History* 352: 1-292. https://doi.org/10.1206/352.1

NESBITT S. J., STOCKER M. R., SMALL B. J. & DOWNS A. 2009. — The osteology and relationships of *Vancleavea campi* (Reptilia: Archosauriformes). *Zoological Journal of the Linnean Society* 157 (4): 814-864. https://doi.org/10.1111/j.1096-3642.2009.00530.x

NESBITT S. J., DESOJO J. B. & IRMIS R. 2013. — *Anatomy, phylogeny and palaeobiology of early archosaurs and their kin.* Geological Society, London, Special Publications 379: 1-7. https://doi.org/10.1144/SP379.21

PADIAN K. & HORNER J. R. 2004. — Physiology, *in* WEISHAMPEL D. B., DODSON P. & OSMOLSKA H. (eds), *The Dinosauria*. 2nd Edition. University of California Press, Berkeley: 660-671.

PADIAN K., RICQLÈS A. DE & HORNER J. 2001. — Dinosaurian growth rates and bird origins. *Nature* 412: 405-408. https://doi.org/10.1038/35086500

PADIAN K., HORNER J. R. & RICQLÈS A. DE 2004. — Growth in small dinosaurs and pterosaurs: the evolution of archosaurian growth strategies. *Journal of Vertebrate Paleontology* 24 (3): 555-571. https://doi.org/bv2hpg

PONCE D. A., CERDA I. A., DESOJO J. B., & NESBITT S. J. 2017. — The osteoderm microstructure in doswelliids and proterochampsids and its implications for palaeobiology of stem archosaurs. *Acta Palaeontologica Polonica* 62 (4): 819-831. https://doi.org/10.4202/app.00381.2017

PONCE D. A., TROTTEYN M. J., CERDA I. A., FIORELLI L. E. & DESOJO J. B. 2021. — Osteohistology and paleobiological inferences of proterochampsids (Eucrocopoda: Proterochampsia) from the Chañares Formation (late Ladinian-early Carnian), La Rioja, Argentina. *Journal of Vertebrate Paleontology* 41 (2): e1926273. https://doi.org/10.1080/02724634.2021.1926273

QUÉMENEUR S., BUFFRÉNIL V. DE & LAURIN M. 2013. — Microanatomy of the amniote femur and inference of lifestyle in limbed vertebrates. *Biological Journal of the Linnean Society* 109 (3): 644-655. https://doi.org/10.1111/bij.12066

RAY S. & CHINSAMY A. 2004. — *Diictodon feliceps* (Therapsida, Dicynodontia): bone histology, growth and biomechanics. *Journal of Vertebrate Paleontology* 24 (1): 180-194. https://doi.org/10.1671/1914-14

RAY S., BOTHA J. & CHINSAMY A. 2004. — Bone histology and growth patterns of some nonmammlian therapsids. *Journal of Vertebrate Paleontology* 24: 634-648. https://doi.org/dfm55f

RAY S., CHINSAMY A. & BANDYOPADHYAY S. 2005. — *Lystrosaurus murrayi* (Therapsida, Dicyndontia): bone histology, growth and lifestyle adaptations. *Palaeontology* 48 (6): 1169-1185. https://doi.org/10.1111/j.1475-4983.2005.00513.x

RAY S., BANDYOPADHYAY S. & BHAWAL D. 2009. — Growth patterns as deduced from bone microstructureof some selected neotherapsids with special emphasis on dicynodonts: phylogenetic implications. *Palaeoworld* 18 (1): 53-66. https://doi.org/10.1016/j.palwor.2008.09.001

REID R. E. H. 1996. — Bone histology of the Cleveland-Lloyd dinosaurs and of dinosaurs in general, Part I. Introduction: introduction to bone tissues. *Brigham Young University Geology Studies* 41: 25-72.

REIG O. A. 1959. — Primeros datos descriptivos sobre nuevos reptiles arcosaurios del Triásico de Ischigualasto (San Juan, Argentina). *Revista de la Asociación Geológica Argentina* 13: 257-270.

REISZ R. R., SCOTT D., SUES H. D., EVANS D. C. & RAATH M. A. 2005. — Embryos of an early Jurassic prosauropod dinosaur and their evolutionary significance. *Science* 309 (5735): 761-764. https://doi.org/10.1126/science.1114942

RICQLÈS A. DE 1976. — On bone histology of fossil and living reptiles, with comments on its functional and evolutionary significance, *in* BELLAIRS A. D'A. & COX C. B. (eds), *Morphology and Biology of Reptiles.* Vol. 1. Linnean Society of London, Academic Press, London: 123-150

RICQLÈS A. DE & BUFFRÉNIL V. DE 2001. — Bone histology, heterochronies and the return of the tetrapods to life, *in* MAZIN J. M. & BUFFRÉNIL V. DE (eds), *Water Where Are We?* Verlag Dr Friedrich Pfeil, Munchen: 95-117.

RICQLES A. DE, MEUNIER F. J., CASTANET J. & FRANCILLON-VIEILLOT E. 1991. — Comparative microstructure of bone, *in* HALL B. K. (ed.), *Bone, Bone Matrix and Bone Specific Products.* Vol. 3. CRC Press, Boca Raton: 1-78.

RICQLÈS A. DE, PADIAN K., HORNER J. & FRANCILLON-VIEILLOT H. 2000. — Palaeohistology of the bones of pterosaurs (Reptilia: Archosauria): anatomy, ontogeny, and biomechanical implications. *Zoological Journal of the Linnean Society* 129 (3): 349-385. https://doi.org/10.1111/j.1096-3642.2000.tb00016.x

RICQLÈS A. DE, PADIAN K. & HORNER J. 2003. — On the bone histology of some Triassic pseudosuchian archosaurs and related taxa. *Annales de Paléontologie* 89 (2): 67-101. https://doi.org/10.1016/S0753-3969(03)00005-3

RICQLÈS A. DE, PADIAN K., KNOLL F. & HORNER J. 2008. — On the origin of high growth rates in archosaurs and their ancient relatives: complementary histological studies on Triassic archosauriforms and the problema of a "phylogenetic signal" in bone histology. *Annales de Paléontologie* 94 (2): 57-76. https://doi.org/10.1016/j.annpal.2008.03.002

ROMER A. S. 1971. — The Chañares (Argentina) Triassic reptile fauna. XI. Two new long- snouted thecodonts, *Chanaresuchus* and *Gualosuchus. Breviora* 379: 1-22.

SÁNCHEZ S., RICQLÈS A. DE, SCHOCH R. R. & STEYER J. S. 2010. — Developmental plasticity of limb bone microstructural organization in *Apateon*: histological evidence of paedomorphic conditions in branchiosaurs. *Evolution & Development* 12 (3): 315-328. https://doi.org/10.1111/j.1525-142X.2010.00417.x

SANDER P. M. & KLEIN N. 2005. — Developmental plasticity in the life history of a prosauropod dinosaur. *Science* 310 (5755): 1800-1802. https://doi.org/10.1126/science.1120125

SERENO P. C. & ARCUCCI A. B. 1990. — The monophyly of the crurotarsal archosaurs and the origin of birds and crocodile ankle joints. *Neues Jahrbuch fur Geologie und Paläontologie Abhandlungen* 180 (1): 21-52. https://doi.org/10.1127/njgpa/180/1990/21

SILL W. D. 1967. — *Proterochampsa barrionuevoi* and the early evolution of the Crocodilia. *Bulletin of the Museum of Comparative Zoology* 135: 415-446.

SMITH-GILL S. J. 1983. — Developmental plasticity: developmental conversión versus phenotypic modulation. *American Zoologist* 23 (1): 47-55. https://doi.org/10.1093/icb/23.1.47

STARCK J. M. & CHINSAMY A. 2002. — Bone microstructure and developmental plasticity in birds and other dinosaurs. *Journal of Morphology* 254 (3): 232-246. https://doi.org/10.1002/jmor.10029

TAYLOR M. A. 2000. — Functional significance of bone ballast in the evolution of buoyancy control strategies by aquatic tetrapods. *Historical Biology* 14 (1-2): 15-31. https://doi.org/10.1080/10292380009380550

TROTTEYN M. J. & EZCURRA M. D. 2020. — Redescription of the holotype of *Chanaresuchus bonapartei* Romer, 1971 (Archosauriformes: Proterochampsidae) from the Upper Triassic rocks of the Chañares Formation of north-western Argentina. *Journal of Systematic Palaeontology* 18 (17): 1415-1443. https://doi.org/10.1080/14772019.2020.1768167

Trotteyn M. J., Arcucci A. B. & Raugust T. 2013. — Proterochampsia: an endemic archosauriform clade from South America, *in* Nesbitt S. J., Desojo J. B. & Irmis R. B. (eds), Anatomy, Phylogeny and Palaeobiology of EarlyArchosaurs and their Kin. *Geological Society, London, Special Publications* 379: 50-90. https://doi.org/10.1144/SP379.23

Veiga F. H., Botha-Brink J., Ribeiro A. M., Ferigolo J. & Soares M. B. 2019. — Osteohistology of the silesaurid Sacisaurus agudoensis from southern Brazil (Late triassic) and implications for growth in early dinosaurs. *Anais da Academia Brasileira de Ciências* 91 (supplement 2): e20180643. https://doi.org/10.1590/0001-3765201920180643

Warshaw J. 2008. — Comparative primate bone microstructure: records of life history, function, and phylogeny, *in* Sargis E. J. & Dagosto M. (eds), *Mammalian Evolutionary Morphology: A Tribute to Frederick S. Szalay*. Springer, Dordrecht: 385-425. https://doi.org/10.1007/978-1-4020-6997-0_18

Werning S. 2013. — *Evolution of Bone Histological Characters in Amniotes, and the Implications for the Evolution of Growth and Metabolism*. PhD Dissertation, University of California, Berkeley, 445 p.

West-Eberhard M. J. 2003. — *Developmental Plasticity and Evolution*. Oxford University Press, Oxford, 814 p. https://doi.org/10.1093/oso/9780195122343.001.0001

Woodward H. N., Horner J. R. & Farlow J. O. 2011. — Osteohistological evidence for determinate growth in the American

alligator. *Journal of Herpetology* 45 (3): 339-342. https://doi.org/10.1670/10-274.1

Woodward H. N., Horner J. R. & Farlow J. O. 2014. — Quantification of intraskeletal histovariability in *Alligator mississippiensis* and implications for vertebrate osteohistology. *PeerJ* 2: e422. https://doi.org/10.7717/peerj.422

Woodward H. N., Freedman-Fowler E. A., Farlow J. O. & Horner J. R. 2015. — *Maiasaura*, a model organism for extinct vertebrate population biology: a large simple statistical assessment of growth dynamics and survivorship. *Paleobiology* 41: 503-527. https://doi.org/10.1017/pab.2015.19

Wynd B. M., Nesbitt S. J., Stocker M. R. & Heckert A. B. 2020. — A Detailed description of *Rugarhynchos sixmilensis*, gen. et comb. nov. (Archosauriformes, Proterochampsia), and cranial convergence in snout elongation across stem and crown archosaurs. *Journal of Vertebrate Paleontology* 39 (6): e1748042. https://doi.org/10.1080/02724634.2019.1748042

Zug G. R. & Rand S. A. 1987. — Estimation of age in nesting female *Iguana iguana*: testing skeletochronology in a tropical lizard. *Amphibia-Reptilia* 8: 237-250. https://doi.org/10.1163/156853887X00289

Zug G. R., Wynn A. H. & Ruckdeschel C. 1986. — Age determination of loggerhead sea turtles, *Caretta caretta*, by incremental growth marks in the skeleton. *Smithsonian Contributions to Zoology* 427: 1-34. https://doi.org/10.5479/si.00810282.427

APPENDIX

Appendix 1. — Inferred lifestyle obtained by the discriminant function A based on Rmin, S, Rmax, MC, Min, OC and SVL (model created by Laurin *et al.* (2004) for lissamphibians). This model was produced by forward selection of variables. Previously performed in amniotes femur by Quémeneur *et al.* (2013) and in ophiacodontids femur by Laurin & Buffrénil (2016). Possible states of lifestyle: **0** = aquatic; **1** = amphibious; **2** = terrestrial. Abbreviations: **MC**, modelled compactness; **Min**, minimun global value; **OC**, observed compactness; **R$_{max}$**, maximun angular value; **R$_{min}$**, minumum angular value; **S**, slope (global value); **SVL**, snout-vent length (cm).

	Tropidosuchus romeri Arcucci, 1990 PVL 4604 femur (this study)	*Clepsydrops* Cope, 1875 (Pelycosauria: Ophiacodontidae) (Laurin & Buffrénil 2016)	*Coleonyx elegans* Gray, 1845 (Squamata: Eublepharidae) (Quémeneur *et al.* 2013)	*Gallotia stehlini* (Schenkel, 1901) (Squamata: Lacertidae) (Quémeneur *et al.* 2013)	0 Aquatic	1 Amphibious	2 Terrestrial
R$_{min}$	0.000	0.000	0.000	0.000	3841.745	–245.782	–174.785
S	0.026	0.012	0.015	0.016	–54.535	161.282	100.756
R$_{max}$	0.858	1.000	1.000	1.000	7.284	43.311	39.007
MC	0.281	0.434	0.384	0.408	6.796	38.465	24.597
Min	0.000	0.007	–0.002	–0.001	–540.124	–26.355	–58.849
OC	0.462	0.434	0.372	0.487	17.891	–13.026	–3.251
SVL	24.40	33.35	7.00	22.00	0.060	0.010	0.011
Constante	–	–	–	–	–272.307	–37.327	–26.839
Inferred lifestyle	0 Terrestrial	2 Terrestrial	2 Terrestrial	2 Terrestrial	–255.828	9.044	14.925 false